



Available online at www.sciencedirect.com

ScienceDirect

Comput. Methods Appl. Mech. Engrg. 390 (2022) 114444

Computer methods in applied mechanics and engineering

www.elsevier.com/locate/cma

Low-order divergence-free approximations for the Stokes problem on Worsey–Farin and Powell–Sabin splits[★]

Maurice Fabien^a, Johnny Guzmán^a, Michael Neilan^{b,*}, Ahmed Zytoon^b

^a Division of Applied Mathematics, Brown University, Providence, RI 02912, USA

^b Department of Mathematics, University of Pittsburgh, Pittsburgh, PA 15260, USA

Received 19 May 2021; received in revised form 16 November 2021; accepted 5 December 2021 Available online 23 December 2021

Abstract

We derive low-order, inf-sup stable and divergence-free finite element approximations for the Stokes problem using Worsey–Farin splits in three dimensions and Powell–Sabin splits in two dimensions. The velocity space simply consists of continuous, piecewise linear polynomials, whereas the pressure space is a subspace of piecewise constants with weak continuity properties at singular edges (3D) and singular vertices (2D). We discuss implementation aspects that arise when coding the pressure space, and in particular, show that the pressure constraints can be enforced at an algebraic level. © 2021 Elsevier B.V. All rights reserved.

Keywords: Divergence-free; Low-order; Worsey-Farin; Powell-Sabin

1. Introduction

The first inf–sup stable finite element spaces that yield divergence-free approximations for incompressible fluid models on simplicial triangulations were given in the classical paper by Scott and Vogelius [1]. Their lowest order pair, defined on a two-dimensional domain, used quartic Lagrange finite elements and piecewise cubic polynomials for the discrete velocity and pressure spaces, respectively; since then, there have been several efforts to find lower order inf–sup stable and conforming finite element spaces that produce divergence-free approximations [2–10].

If we confine ourselves to Lagrange elements for the velocity space, then a reduction of polynomial degree, while preserving stability, can be done on certain splits (i.e., refinements) of a simplicial mesh. For example, Zhang proved stability of the three-dimensional cubic–quadratic pair on Alfeld splits [5], and stability of the three-dimensional quadratic–linear pair on Worsey–Farin splits [10]. On the other hand, Zhang suggests that piecewise linear Lagrange elements for the velocity are unstable on Worsey–Farin splits [10, p. 244]. One of the main objectives of this paper is to show that indeed the linear case is stable if coupled with the correct pressure space.

E-mail addresses: fabien@brown.edu (M. Fabien), johnny_guzman@brown.edu (J. Guzmán), neilan@pitt.edu (M. Neilan), AMZ56@pitt.edu (A. Zytoon).

[☆] This work was partial supported by the National Science Foundation, USA through grants DMS-1933083 (Guzmán) and DMS-2011733 (Neilan and Zytoon).

^{*} Corresponding author.

The main goal of this paper is to construct inf-sup stable and divergence-free pairs on simplicial (split) meshes using a linear-constant velocity-pressure pair on Worsey-Farin splits (3D) and Powell-Sabin splits (2D). As far as we are aware, this is the first three-dimensional pair with these properties using linear Lagrange elements for the discrete velocity space. The main driver of our construction is an explicit characterization of the divergence operator acting on the Lagrange finite element space developed in [11,12]. Such characterizations naturally lead to the definitions of the discrete pressure space. In particular, the pressure space is a subspace of piecewise constants with weak continuity constraints on singular edges (Worsey-Farin) and singular vertices (Powell-Sabin).

Our results in two dimensions are similar to those in [6], where Zhang showed stability of a Stokes pair with linear Lagrange elements for the velocity space on Powell–Sabin splits. However, the pressure space was not characterized in [6] and as a result, a pressure basis is not explicitly constructed. Due to the implicit definition of the pressure space, one is forced to solve the resulting algebraic system by the iterated penalty method (IPM). In contrast, the explicit characterization of the pressure space we provide opens the door to a library of solvers based on the standard mixed formulation.

An advantage of the proposed schemes is their low computational cost and simple velocity spaces, which are supported in finite element software libraries. On the other hand, the discrete pressure spaces are subspaces of piecewise constants with weak continuity properties at singular edges and singular vertices; these spaces are nonstandard, and in particular are not readily available on computational software packages. Nonetheless, we show that these weak continuity properties can be enforced entirely at the algebraic level. One can simply form the algebraic saddle point problem using the full (unstable) linear-constant pair, and then perform elementary row and column operations to this system to enforce the weak continuity constraint. As a result, the proposed discretizations can be implemented on standard finite element software packages (e.g., FEniCS).

We note that degrees of freedom and commuting projections were given in [11,12]. In fact, an entire exact sequence of spaces were presented. However, stability (e.g., inf–sup stability) was not shown, which is something we carry out here.

Moreover, we provide numerical experiments to validate our theoretical results. In particular, we show that the computed solution is satisfying the standard error estimates in mixed formulation. Also, we provide a time comparison between the stiffness matrix modification method described above and the iterated penalty method.

The paper is organized as follows. In the next section we provide the notation used throughout the paper and introduce the Stokes problem. Section 3 proves the inf-sup stability of a low-order finite element pair on Powell-Sabin splits. In Section 4 we prove stability of the analogous three-dimensional pair on Worsey-Farin splits. In Section 5 we discuss implementation aspects on Powell-Sabin splits and in Section 6 we do the same for Worsey-Farin splits. Finally, in Section 7 we provide numerical experiments.

2. Preliminaries

In this section we develop basic notation that we use throughout the paper. We provide this in the following list:

- \mathcal{T}_h is a shape-regular, simplicial triangulation of a contractible polytope $\Omega \subset \mathbb{R}^d$ (d=2,3).
- $h_T = \operatorname{diam}(T)$ for all $T \in \mathcal{T}_h$ and $h = \max_{T \in \mathcal{T}_h} h_T$.
- For an *n*-dimensional simplex S ($n \leq d$) and $m \in \{0, \ldots, n\}$, denote by $\Delta_m(S)$ the set of *m*-dimensional simplices of S. Likewise, for a simplicial triangulation Q_h , we let $\Delta_m(Q_h)$ denote the set of *m*-dimensional simplices in Q_h .
- $\mathcal{P}_r(S)$ denotes the space of polynomials of degree $\leq r$ with domain S. Analogous spaces of vector-valued functions are given in boldface, e.g., $\mathcal{P}_r(S) = [\mathcal{P}_r(S)]^d$.
- We define the following function spaces on Ω :

$$\begin{split} L^2(\Omega) &:= \{ w : \Omega \mapsto \mathbb{R} : \ \|w\|_{L^2(\Omega)} := (\int_{\Omega} |w|^2)^{1/2} < \infty \}, \\ H^m(\Omega) &:= \{ w : \Omega \mapsto \mathbb{R} : \ \|w\|_{H^m(\Omega)} := (\sum_{|\beta| \le m} \|D^\beta w\|_{L^2(\Omega)}^2)^{1/2} < \infty \}, \end{split}$$

and the spaces with boundary conditions:

$$\mathring{L}^{2}(\Omega) := \{ w \in L^{2}(\Omega) : \int_{\Omega} w = 0 \},$$

$$\mathring{H}^{m}(\Omega) := \{ w \in H^{m}(\Omega) : D^{\beta} w |_{\partial \Omega} = 0, \forall \beta : |\beta| < m-1 \}.$$

Analogous vector-valued function spaces are denoted in boldface, e.g., $\mathbf{H}^1(\Omega) = [H^1(\Omega)]^d$.

• For a simplicial triangulation Q_h , we define the spaces of piecewise polynomials

$$\mathfrak{P}_{k}(\mathfrak{Q}_{h}) = \prod_{K \in \mathfrak{Q}_{h}} \mathfrak{P}_{k}(K), \qquad \mathfrak{P}_{k}(\mathfrak{Q}_{h}) = \prod_{K \in \mathfrak{Q}_{h}} \mathfrak{P}_{k}(K), \qquad \mathfrak{P}_{k}^{c}(\mathfrak{Q}_{h}) = \mathfrak{P}_{k}(\mathfrak{Q}_{h}) \cap \mathbf{H}^{1}(D),
\mathring{\mathfrak{P}}_{k}(\mathfrak{Q}_{h}) = \mathfrak{P}_{k}(\mathfrak{Q}_{h}) \cap \mathring{L}^{2}(D), \qquad \mathring{\mathfrak{P}}_{k}^{c}(\mathfrak{Q}_{h}) = \mathfrak{P}_{k}(\mathfrak{Q}_{h}) \cap \mathring{\mathbf{H}}^{1}(D),$$

$$\mathring{\mathcal{P}}_k(\Omega_h) = \mathcal{P}_k(\Omega_h) \cap \mathring{L}^2(D), \qquad \mathring{\mathcal{P}}_k^c(\Omega_h) = \mathcal{P}_k(\Omega_h) \cap \mathring{\boldsymbol{H}}^1(D),$$

where $\bar{D} = \bigcup_{K \in \mathcal{Q}_h} \bar{K}$. Thus $\mathring{\mathcal{P}}_k(\mathcal{Q}_h)$ consists of piecewise polynomials of degree $\leq k$ with respect to the triangulation Ω_h with mean zero, and $\mathring{\mathcal{P}}_k^c(\Omega_h)$ is the space of continuous, piecewise polynomials of degree $\leq k$ with vanishing trace (i.e., the kth degree vector-valued Lagrange finite element space).

• The constant C denotes a generic positive constant, independent of the mesh parameter h.

2.1. The Stokes problem

The Stokes equations defined on a polygonal domain $\Omega \subset \mathbb{R}^d$ with Lipschitz continuous boundary $\partial \Omega$ is given by the system of equations

$$-\nu\Delta u + \nabla p = f \quad \text{in } \Omega, \tag{2.1a}$$

$$\operatorname{div} \mathbf{u} = 0 \qquad \text{in } \Omega, \tag{2.1b}$$

$$\mathbf{u} = 0 \quad \text{on } \partial \Omega.$$
 (2.1c)

where the velocity $\mathbf{u} = (u_1, \dots, u_d)^\mathsf{T}$ and pressure p are functions of $\mathbf{x} = (x_1, \dots, x_d)^\mathsf{T}$, and ∇ , Δ denote the gradient operator and vector Laplacian operator with respect to x respectively. In (2.1a), ν is the viscosity.

The weak formulation for (2.1) reads: Find $(\boldsymbol{u}, p) \in \mathring{\boldsymbol{H}}^1(\Omega) \times \mathring{L}^2(\Omega)$ such that $\forall (\boldsymbol{v}, q) \in \mathring{\boldsymbol{H}}^1(\Omega) \times \mathring{L}^2(\Omega)$ we have

$$\nu \int_{\Omega} \nabla \boldsymbol{u} : \nabla \boldsymbol{v} - \int_{\Omega} (\operatorname{div} \boldsymbol{v}) p = \int_{\Omega} \boldsymbol{f} \cdot \boldsymbol{v},$$

$$\int_{\Omega} (\operatorname{div} \boldsymbol{u}) q = 0.$$
(2.2a)

It is well known that the problem (2.2) has a unique solution [13].

Let $\mathring{V}_h \times \mathring{Y}_h \subset H^1_0(\Omega) \times L^2_0(\Omega)$ be a conforming and finite dimensional pair. Then the finite element method for (2.1), based on the standard velocity-pressure formulation, seeks $(u_h, p_h) \in \mathring{V}_h \times \mathring{Y}_h$ such that $\forall (v, q) \in \mathring{V}_h \times \mathring{Y}_h$

$$\nu \int_{\Omega} \nabla \boldsymbol{u}_{h} : \nabla \boldsymbol{v} - \int_{\Omega} (\operatorname{div} \boldsymbol{v}) p_{h} = \int_{\Omega} \boldsymbol{f} \cdot \boldsymbol{v},$$

$$\int_{\Omega} (\operatorname{div} \boldsymbol{u}_{h}) q = 0.$$
(2.3a)

The discrete problem (2.3) is well-posed if and only if the pair satisfies the inf-sup condition

$$\sup_{0\neq \pmb{v}\in\mathring{V}_h}\frac{\int_{\varOmega}(\mathrm{div}\,\pmb{v})q}{\|\nabla\pmb{v}\|_{L^2(\varOmega)}}\geq \beta\|q\|_{L^2(\varOmega)}\qquad \forall q\in\mathring{Y}_h,$$

for some $\beta > 0$.

3. Inf-sup stability on Powell-Sabin triangulations

Let \mathcal{T}_h be a simplicial, shape-regular triangulation of $\Omega \subset \mathbb{R}^2$. The Powell–Sabin refinement of \mathcal{T}_h , denoted by \mathcal{T}_h^{PS} is obtained by the following procedure [14]. First connect the incenter of each triangle $T \in \mathcal{T}_h$ with its three vertices. Next, the incenters of each adjacent pair of triangles are connected with an edge. If T has a boundary edge, then the midpoint of the boundary edge is connected to the incenter of T. Thus, this procedure splits each triangle in \mathcal{T}_h into six subtriangles; cf. Fig. 1. We set

$$T^{\mathrm{PS}} = \{ K \in \mathfrak{T}_h^{\mathrm{PS}} : K \subset \bar{T} \}.$$

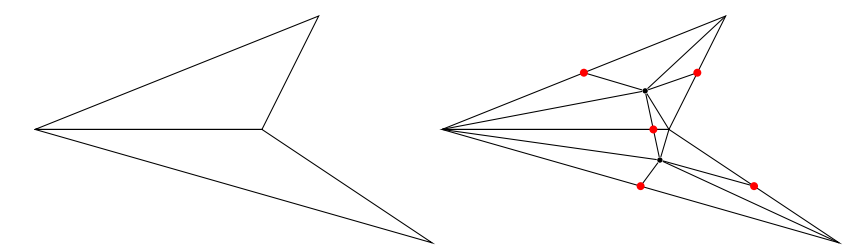


Fig. 1. Two triangles in the mesh \mathfrak{T}_h (left) and their Powell–Sabin refinement (right). The singular vertices in the Powell–Sabin refinement are depicted in red.

Remark 3.1. The Powell–Sabin refinement is defined via the incenter of each triangle; this choice ensures that the line connecting these points intersects the common edge of two macro triangles [15]. We will refer to such interior points of the macro triangulation as split points, as is commonly done in the literature. Other choices of split points can be made as long as the line intersecting them intersect the common edge [16]. The theoretical arguments will remained unchanged. However, for the sake of concreteness, we assume that the split points in the Powell–Sabin refinement are chosen as the incenters.

One feature of the Powell–Sabin triangulation is the presence of singular vertices.

Definition 3.2. We say that a vertex in a simplicial triangulation is *singular* if the edges meeting at the vertex fall on exactly two straight lines.

Let \mathcal{S}_h^I and \mathcal{S}_h^B denote the sets of interior and boundary singular vertices in \mathfrak{T}_h^{PS} , respectively, and set $\mathcal{S}_h = \mathcal{S}_h^I \cup \mathcal{S}_h^B$. Note that the cardinalities of the sets \mathcal{S}_h^I and \mathcal{S}_h^B correspond to the number of interior and boundary edges in \mathcal{T}_h , respectively. For $z \in \mathcal{S}_h^I$, we denote by $\mathcal{T}_z \subset \mathcal{T}_h^{PS}$ the set of four triangles that have z as a vertex. We write $\mathcal{T}_z = \{K_z^{(1)}, K_z^{(2)}, K_z^{(3)}, K_z^{(4)}\}$ with $K_z^{(j)} \in \mathcal{T}_h^{PS}$, labeled such that $K_z^{(j)}$ and $K_z^{(j+1)}$ have a common edge. Likewise, for $z \in \mathcal{S}_h^B$, we set $\mathcal{T}_z = \{K_z^{(1)}, K_z^{(2)}\} \subset \mathcal{T}_h^{PS}$ to denote the two triangles that have z as a vertex. We set $n_z = |\mathcal{T}_z|$, i.e., $n_z = 4$ if $z \in \mathcal{S}_h^I$ and $n_z = 2$ if $z \in \mathcal{S}_h^B$.

3.1. Finite element spaces on Powell-Sabin triangulations

It is well known that, on singular vertices, the divergence operator acting on the Lagrange finite element space has "weak continuity properties"; the precise meaning of this statement is provided in the following lemma. Its proof can be found in, e.g., [1,17].

Lemma 3.3. For $z \in S_h$, and piecewise smooth function q, define

$$\theta_{z}(q) := \left\{ \begin{array}{ll} q|_{K_{z}^{(1)}}(z) - q|_{K_{z}^{(2)}}(z) + q|_{K_{z}^{(3)}}(z) - q|_{K_{z}^{(4)}}(z) & z \in \mathbb{S}_{h}^{I}, \\ q|_{K_{z}^{(1)}}(z) - q|_{K_{z}^{(2)}}(z) & z \in \mathbb{S}_{h}^{B}. \end{array} \right.$$

Then there holds $\theta_z(\text{div } \mathbf{v}) = 0$ for all $\mathbf{v} \in \mathring{\mathbf{P}}_k^c(\mathbb{T}_h^{PS})$.

Based on Lemma 3.3, and on a discrete de Rham complex, divergence-free finite element pairs for the Stokes problem have been constructed and analyzed in [6,11] on Powell–Sabin triangulations. Here, we focus on the lowest-order case, where the velocity space is the linear Lagrange space, and the pressure space is a subspace of piecewise constants with a weak continuity property at singular vertices. We first define the spaces without boundary conditions and then the ones with boundary conditions.

$$\begin{aligned} \boldsymbol{V}_h^{\text{PS}} &:= \boldsymbol{\mathcal{P}}_1^c(\boldsymbol{\mathcal{T}}_h^{\text{PS}}), \\ \boldsymbol{Y}_h^{\text{PS}} &:= \{q \in \mathcal{P}_0(\boldsymbol{\mathcal{T}}_h^{\text{PS}}): \ \theta_z(q) = 0 \ \forall z \in \mathcal{S}_h^I\}. \end{aligned}$$

We now define an intermediate pressure space

$$\hat{Y}_h^{\text{PS}} := \{ q \in \mathcal{P}_0(\mathcal{T}_h^{\text{PS}}) : \theta_z(q) = 0 \ \forall z \in \mathcal{S}_h \}.$$

The spaces with boundary conditions are

$$\mathring{\boldsymbol{V}}_{h}^{\mathrm{PS}} := \boldsymbol{V}_{h}^{\mathrm{PS}} \cap \mathring{\boldsymbol{H}}^{1}(\Omega),
\mathring{Y}_{h}^{\mathrm{PS}} := \mathring{Y}_{h}^{\mathrm{PS}} \cap \mathring{L}^{2}(\Omega).$$

3.2. Stability of
$$\mathring{\boldsymbol{V}}_h^{\text{PS}} \times \mathring{\boldsymbol{Y}}_h^{\text{PS}}$$

The stability of the pair $\mathring{V}_{h}^{PS} \times \mathring{Y}_{h}^{PS}$ is implicitly shown in [18, Lemma 3.3]. Here we give more details.

Theorem 3.4. There holds div $\mathring{V}_h^{PS} \subseteq \mathring{Y}_h^{PS}$. In addition, the pair $\mathring{V}_h^{PS} \times \mathring{Y}_h^{PS}$ is an inf–sup stable pair for the Stokes problem, i.e.,

$$\sup_{0\neq \pmb{v}\in\mathring{V}_h^{\mathrm{PS}}}\frac{\int_{\varOmega}(\mathrm{div}\,\pmb{v})q}{\|\nabla\pmb{v}\|_{L^2(\varOmega)}}\geq \beta\|q\|_{L^2(\varOmega)}\quad\forall q\in\mathring{Y}_h^{\mathrm{PS}},$$

for some $\beta > 0$ independent of the mesh parameter h.

Proof. The inclusion div $\mathring{V}_h^{\mathrm{PS}} \subseteq \mathring{Y}_h^{\mathrm{PS}}$ follows from Lemma 3.3 and the definition of \mathring{Y}_h^{PS} . For $T \in \mathcal{T}_h$, let $z \in \mathcal{S}_h$ with $z \subset \bar{T}$ and let $\{K_1, K_2\} \subset T^{\mathrm{PS}}$ be the two triangles in the Powell–Sabin refinement of T that have z as a vertex. Let v_i be the outward normal of K_i perpendicular to the common edge $\partial K_1 \cap \partial K_2$; see Fig. 2. We define the jump operator of a function p defined on T at z as

$$[\![p]\!](z) = p|_{K_1}(z)\mathbf{v}_1 + p|_{K_2}(z)\mathbf{v}_2.$$

Note that if $T_1, T_2 \in \mathcal{T}_h$ are two macro triangles with a common point $z \in \mathcal{S}_h$ then $\theta_z(p) = 0$ if and only if $[p|_{T_1}](z) = [p|_{T_2}](z)$. In particular, a piecewise constant function p with zero mean belongs to the space \mathring{Y}_h^{PS} if and only if [p](z) is single-valued for all $z \in S_h$.

For each $T \in \mathcal{T}_h$, let T^A denote the local triangulation of T consisting of three triangles, obtained by connecting the vertices of T with its incenter, which is known as the Clough-Tocher or Alfeld split of T. Let $q \in \mathring{Y}_h^{PS}$, and let $\mathbf{w} \in \mathring{\mathbf{H}}^1(\Omega)$ satisfy div $\mathbf{w} = q$ and $\|\nabla \mathbf{w}\|_{L^2(\Omega)} \le C \|q\|_{L^2(\Omega)}$. Set $\mathbf{w}_h \in \mathring{\mathcal{P}}_1(\mathfrak{T}_h)$ to be the Scott-Zhang interpolant [19] of \boldsymbol{w} with respect to \mathfrak{I}_h . By [11, Lemma 10], there exists a unique $\boldsymbol{v} \in \mathring{\boldsymbol{V}}_h^{PS}$ such that

$$\begin{split} & \boldsymbol{v}(a) = \boldsymbol{w}_h(a) & \forall a \in \Delta_0(\mathfrak{T}_h), \\ & \int_e (\boldsymbol{v} \cdot \boldsymbol{n}_e) = \int_e (\boldsymbol{w} \cdot \boldsymbol{n}_e) & \forall e \in \Delta_1(\mathfrak{T}_h), \\ & \| \operatorname{div} \boldsymbol{v} \| (z) = \| q \| (z) & \forall z \in \mathbb{S}_h, \\ & \int_T (\operatorname{div} \boldsymbol{v}) p = \int_T q p & \forall p \in \mathcal{P}_0(T^{\mathcal{A}}) \cap L_0^2(T), \forall T \in \mathfrak{T}_h, \end{split}$$

where n_e is a unit vector normal to e. Integration-by-parts shows $\int_T \text{div } \boldsymbol{v} = \int_T \text{div } \boldsymbol{v} = \int_T q$, and therefore, by [11, Lemma 11], there holds div v = q. A standard scaling argument, and using the H^1 -stability of the Scott-Zhang interpolant, then shows $\|\nabla v\|_{L^2(\Omega)} \leq C \|q\|_{L^2(\Omega)}$. \square

4. Inf-sup stability on Worsey-Farin splits

Let \mathcal{T}_h be a simplicial triangulation of a polyhedral domain $\Omega \subset \mathbb{R}^3$. The Worsey–Farin triangulation $\mathcal{T}_h^{\mathrm{WF}}$ is obtained by splitting each tetrahedron into twelve sub-tetrahedra by the following procedure [20] (cf. Fig. 3). Similar to the Powell–Sabin case, for each $T \in \mathcal{T}_h$, we connect the incenter (which we refer to as an interior split point) of T to its vertices. Next, the incenters of neighboring pairs of tetrahedra are connected with a line. This creates a face split point (a vertex) on each face of F of T which we denote by m_F . If T has a boundary face, then

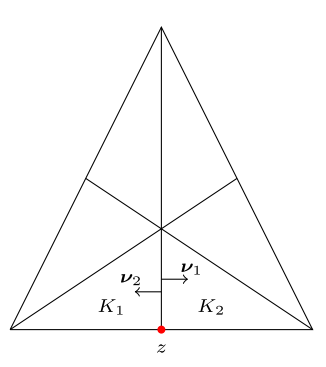


Fig. 2. The Powell-Sabin split of a single triangle.

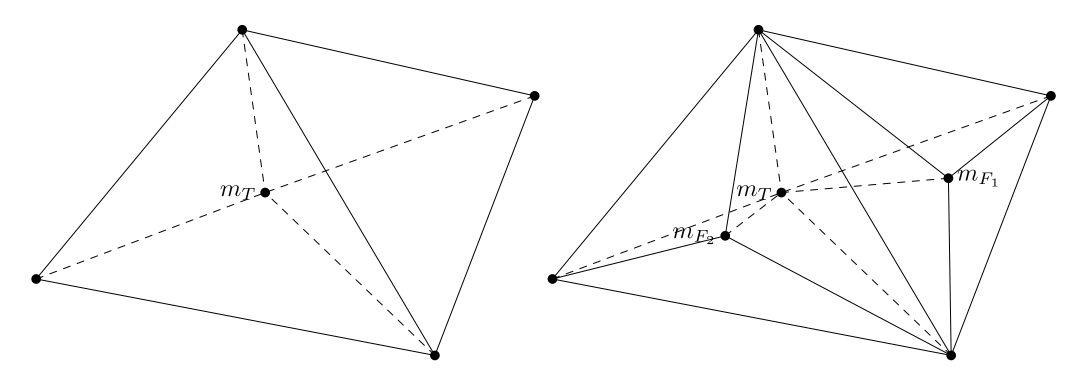


Fig. 3. Representation of a Alfeld split TA (left) and Worsey-Farin split TWF (right) with two faces shown. Solid lines denote external edges of the split, whereas dashed lines denote internal edges. The internal split point is m_T , whereas m_{F_1} and m_{F_2} are face split points.

we connect the incenter of T to the barycenter of the face by a line. Finally, the face split points are connected to the vertices of the face. For each $T \in \mathcal{T}_h$, we denote by T^{WF} the triangulation resulting from local Worsey–Farin refinement of T, i.e.,

$$T^{\mathrm{WF}} = \{ K \in \mathfrak{T}_h^{\mathrm{WF}} : \ K \subset \bar{T} \}.$$

Remark 4.1. Similar to the Powell–Sabin refinement (cf. Remark 3.1), taking the interior split point as the incenter in the Worsey-Farin refinement guarantees that the line intersecting adjacent interior split points intersects a common face. Provided that the refinement is shape-regular and the local triangulations are quasi-uniform, the arguments and analysis given below hold for arbitrary split points provided that the line intersecting them intersect the common face.

Definition 4.2. An edge in a 3D simplicial triangulation is called *singular* if the faces meeting at the edge fall on exactly two planes.

By construction, the Worsey-Farin triangulation contains many singular edges; for each face in the unrefined

triangulation \mathfrak{I}_h , there are three associated singular edges in $\mathfrak{I}_h^{\mathrm{WF}}$. Let $\mathcal{E}_h^{\mathrm{S}}$ denote the set of singular edges in $\mathfrak{I}_h^{\mathrm{WF}}$, and let $\mathcal{E}_h^{\mathrm{S},l}$ and $\mathcal{E}_h^{\mathrm{S},B}$ denote the sets of interior and boundary singular edges, respectively. For each $e \in \mathcal{E}_h^{\mathrm{S}}$, let $\mathfrak{I}_e = \{K_e^{(1)}, \ldots, K_e^{(n_e)}\}$ denote the set of tetrahedra that have e as an edge. Here, $n_e = 4$ if e is an interior edge, and $n_e = 2$ if e is a boundary edge. We assume the tetrahedra are labeled such that $K_e^{(j)}$ and $K_e^{(j+1)}$ share a common face.

4.1. Finite element spaces on Worsey-Farin triangulations

Similar to the two-dimensional case, the divergence operator acting on the Lagrange finite element space has weak continuity properties on singular edges (cf. [12], [21, Lemma 5.7.4]).

Lemma 4.3. For $e \in \mathcal{E}_h^{\mathbb{S}}$, and a piecewise smooth function q, define

$$\theta_e(q) = \left\{ \begin{array}{ll} q_e^{(1)}|_e - q_e^{(2)}|_e + q_e^{(3)}|_e - q_e^{(4)}|_e & e \in \mathcal{E}_h^{8,I}, \\ q_e^{(1)}|_e - q_e^{(2)}|_e & e \in \mathcal{E}_h^{8,B}, \end{array} \right.$$

where $q_e^{(j)} = q|_{K^{(j)}}$. Then there holds $\theta_e(\text{div } \mathbf{v}) = 0$ for all $\mathbf{v} \in \mathring{\mathcal{P}}_k^c(\mathcal{T}_h^{\text{WF}})$.

Analogous to the Powell-Sabin case, we define the finite element spaces to discretize the Stokes problem on Worsey-Farin splits. We first define the spaces without boundary conditions

$$\begin{aligned} & \boldsymbol{V}_h^{\text{WF}} = \boldsymbol{\mathcal{P}}_1^c(\boldsymbol{\mathcal{T}}_h^{\text{WF}}), \\ & \boldsymbol{Y}_h^{\text{WF}} = \{ \boldsymbol{q} \in \boldsymbol{\mathcal{P}}_0(\boldsymbol{\mathcal{T}}_h^{\text{WF}}) : \ \boldsymbol{\theta}_e(\boldsymbol{q}) = 0 \ \forall \boldsymbol{e} \in \boldsymbol{\mathcal{E}}_h^{\boldsymbol{\mathcal{S}},I} \}. \end{aligned}$$

Then, we define an intermediate pressure space

$$\hat{Y}_h^{\text{WF}} = \{ q \in \mathcal{P}_0(\mathcal{T}_h^{\text{WF}}) : \theta_e(q) = 0 \ \forall e \in \mathcal{E}_h^{\mathcal{S}} \}.$$

We now define the spaces with boundary conditions

$$\mathring{\boldsymbol{V}}_{h}^{\text{WF}} = \boldsymbol{V}_{h}^{\text{WF}} \cap \mathring{\boldsymbol{H}}^{1}(\Omega),
\mathring{\boldsymbol{Y}}_{h}^{\text{WF}} = \hat{\boldsymbol{Y}}_{h}^{\text{WF}} \cap \mathring{\boldsymbol{L}}^{2}(\Omega).$$

4.2. Stability of
$$\mathring{\boldsymbol{V}}_h^{\text{WF}} \times \mathring{\boldsymbol{Y}}_h^{\text{WF}}$$

In this section, we show the pair $\mathring{V}_h^{\mathrm{WF}} \times \mathring{Y}_h^{\mathrm{WF}}$ is inf-sup stable. First we introduce some notation. Let $T \in \mathcal{T}_h$, and let T^A denote the local triangulation of T consisting of four tetrahedra, obtained by connecting the vertices of T with its incenter, i.e., T^A denotes the Alfeld split of T [15,22]. For a face $F \subset T$, denote by F^{CT} the set of three triangles formed from F by the Worsey-Farin refinement, i.e., F^{CT} is the Clough-Tocher refinement of F [15]. We denote by $\Delta_1^I(F^{\mathrm{CT}})$ the set of three interior edges in F^{CT} , and let $e_F \in \Delta_1^I(F^{\mathrm{CT}})$ denote an arbitrary, fixed interior edge of F^{CT} .

To prove inf-sup stability we will need the degrees of freedom of these space. In order to define degrees of freedom of the above spaces we need to define a jump on singular edges.

Definition 4.4. Let $T \in \mathcal{T}_h$, let F be one of its faces, and let $e \in \mathcal{E}_h^S$ be a singular edge with $e \subset F$. Let $K_1, K_2 \in T^{\mathrm{WF}}$ be the two micro-tetrahedra that have e as an edge. Let v_i be outward unit normal to K_i that is perpendicular to the common face $\partial K_1 \cap \partial K_2$. Then the jump of a piecewise smooth function p defined on T across e is defined as

$$[\![p]\!]_e = p^{(1)}|_e \mathbf{v}_1 + p^{(2)}|_e \mathbf{v}_2, \text{ where } p^{(i)} = p|_{K_i}.$$

Remark 4.5. Let $T_1, T_2 \in \mathcal{T}_h$ and let $e \in \mathcal{E}_h^{\mathbb{S}}$ be common to both T_1 and T_2 then it is clear that $\theta_e(p) = 0$ if and only if $[\![p]_{T_1}]\!]_e = [\![p]_{T_2}]\!]_e$, that is, a piecewise constant function p belongs to the space \hat{Y}_h^{WF} if and only if $[\![p]\!]_e$ is single-valued for all $\mathcal{E}_h^{\mathbb{S}}$.

We now state the degrees of freedom (DOFs) for the spaces $\mathring{V}_h^{\text{WF}}$ and $\mathring{Y}_h^{\text{WF}}$. We first define the local DOFs. The proofs of the following two lemmas are particular cases of [12, Lemmas 5.10–5.11]. For completeness, we provide the proofs of the results.

Lemma 4.6. A function $q \in \mathcal{P}_0(T^{WF})$ is uniquely determined by

$$\int_{e} \llbracket q \rrbracket_{e} \qquad \forall e \in \Delta_{1}^{I}(F^{\text{CT}}) \setminus \{e_{F}\}, \ \forall F \in \Delta_{2}(T), \qquad (8 \ DOFs), \tag{4.1a}$$

$$\int_{T} qp \qquad \forall p \in \mathcal{P}_{0}(T^{A}), \tag{4.1b}$$

where the integral of $[q]_e$ is done component-wise.

Proof. The dimension of $\mathcal{P}_0(T^{WF})$ is 12 (the number of tetrahedra in T^{WF}), so it suffices to show that if $q \in \mathcal{P}_0(T^{\mathrm{WF}})$ vanishes on the DOFs (4.1), then $q \equiv 0$. For a face $F \in \Delta_2(T)$, let Q_1, Q_2, Q_3 be the three triangles of the Clough-Tocher split F^{CT} with respect to the split point m_F . Without loss of generality, assume that $e_F = \partial Q_1 \cap \partial Q_2$. By (4.1a), noting that q is piecewise constant, we see that $q|_{Q_2}(m_F) = q|_{Q_1}(m_F)$ and $q|_{Q_2}(m_F)=q|_{Q_3}(m_F)$. By transitivity, we have $[\![q]\!]_e=0$ for all $e\in\Delta_1^I(F^{\rm CT})$, and therefore, since $F\in\Delta_2(T)$ was arbitrary and q is piecewise constant, we conclude $q \in \mathcal{P}_0(T^A)$. The DOFs (4.1b) then yield $q \equiv 0$. \square

Lemma 4.7. A function $\mathbf{v} \in \mathfrak{P}_1^c(T^{\mathrm{WF}})$ is uniquely determined by the values

$$\mathbf{v}(a) \qquad \forall a \in \Delta_0(T), \tag{4.2a}$$

$$\int_{F} (\boldsymbol{v} \cdot \boldsymbol{n}_{F}) \qquad \forall F \in \Delta_{2}(T), \tag{4.2b}$$

$$\int [[\operatorname{div} \mathbf{v}]]_e \qquad \forall e \in \Delta_1^I(F^{\operatorname{CT}}) \setminus \{e_F\}, \ \forall F \in \Delta_2(T), \qquad (8 \ DOFs), \tag{4.2c}$$

$$\int_{F} (\boldsymbol{v} \cdot \boldsymbol{n}_{F}) \qquad \forall F \in \Delta_{2}(T), \qquad (4 \text{ DOFs}), \qquad (4.2b)$$

$$\int_{e} [[\operatorname{div} \boldsymbol{v}]]_{e} \qquad \forall e \in \Delta_{1}^{I}(F^{\text{CT}}) \setminus \{e_{F}\}, \ \forall F \in \Delta_{2}(T), \qquad (8 \text{ DOFs}), \qquad (4.2c)$$

$$\int_{T} (\operatorname{div} \boldsymbol{v}) p \qquad \forall p \in \mathring{\mathcal{V}}_{0}(T) := \mathcal{P}_{0}(T^{\text{A}}) \cap L_{0}^{2}(T), \qquad (3 \text{ DOFs}). \qquad (4.2d)$$

Here, the integral of $[\![\operatorname{div} \boldsymbol{v}]\!]_e$ is performed component-wise, and \boldsymbol{n}_F is the outward unit normal of ∂T restricted to F.

Proof. There are 9 vertices in T^{WF} . Therefore dim $\mathcal{P}_1^c(T^{WF}) = 9 \cdot 3 = 27$, which is the number of DOFs in (4.2). We show that $\mathbf{v} \in \mathcal{P}_1^c(T^{\mathrm{WF}})$ vanishes on (4.2) if and only if $\mathbf{v} \equiv 0$. As an intermediate step, and to show that the DOFs induce continuity in the global space, we show that if $\mathbf{v} \in \mathcal{P}_1^c(T^{\mathrm{WF}})$ vanishes on (4.2a)–(4.2c) restricted to a single face $F \subset \partial T$, then $\mathbf{v}|_F = 0$.

Fix $F \subset \partial T$, and suppose that $\mathbf{v} \in \mathcal{P}_1^c(T^{\mathrm{WF}})$ vanishes on (4.2a)–(4.2c) restricted to F. Using (4.2a), we have $v|_e = 0$ for all $e \in \Delta_1(F)$, and therefore, due to (4.2b), there holds $v \cdot n_F|_F = 0$. We now show that the tangential component $\mathbf{v}_F := \mathbf{n}_F \times \mathbf{v} \times \mathbf{n}_F$ vanishes on the boundary of T.

Let $\mu \in \mathring{\mathbb{P}}_1^c(T^A) \subset \mathring{\mathbb{P}}_1^c(T^{WF})$ be the piecewise linear hat function with respect to the incenter of T. Let $K \in T^A$ be the tetrahedron in the Alfeld refinement of T such that $F \subset \partial K$. Then, because $\mathbf{v} \cdot \mathbf{n}_F|_F = 0$, there holds $\mathbf{v} \cdot \mathbf{n}_F|_K = c\mu$ for some $c \in \mathbb{R}$. The DOFs (4.2c) and the arguments in the proof of Lemma 4.6 shows that div $\mathbf{v}|_F$ is continuous on each $F \in \Delta_2(T)$. Write the tangential divergence as $\operatorname{div}_F \mathbf{v}_F = \operatorname{div} \mathbf{v}|_F - \mathbf{n}_F \cdot \operatorname{\mathbf{grad}}(\mathbf{v} \cdot \mathbf{n}_F)|_F$. Since $n_F \cdot \operatorname{grad}(v \cdot n_F) = cn_F \cdot \operatorname{grad}(\mu|_F)$, and $\operatorname{grad}(\mu|_F)$ is constant on F, we conclude that $\operatorname{div}_F v_F$ is continuous

Next, let $\mu_F \in \mathring{\mathcal{P}}_1(F^{\text{CT}})$ be the hat function satisfying $\mu_F(m_F) = 1$ where we recall m_F is the face split point of F induced by the Worsey-Farin refinement. Because $v_F|_{\partial F}=0$, we may write $v_F|_F=c_F\mu_F$ for some constant c_F . Then $\operatorname{div}_F v_F|_F = c_F \cdot \operatorname{grad}_F \mu_F$ is continuous, and therefore $c_F \equiv 0$. Thus, $v_F|_F = 0$ and we conclude $v|_F = 0$.

Thus, we conclude that if $\mathbf{v} \in \mathcal{P}_1^c(T^{\mathrm{WF}})$ vanishes on (4.2), then $\mathbf{v}|_{\partial T} = 0$. Due to (4.2c)–(4.2d), integrationby-parts, and Lemma 4.6, there holds div v = 0. Because $v|_{\partial T} = 0$, we write $v = c\mu$ for some $c \in \mathbb{R}^3$. Then div $\mathbf{v} = \mathbf{c} \cdot \operatorname{\mathbf{grad}} \mu = 0$ in T. This implies $\mathbf{c} = 0$, and so $\mathbf{v} \equiv 0$. \square

Remark 4.8. Lemmas 4.6 and 4.7 induce the global spaces \hat{Y}_h^{WF} and V_h^{WF} , respectively. To see this, first note the proof of Lemma 4.6 shows that if a piecewise constant function is single-valued for two edges of an interior face, then it is single-valued on all three edges by transitivity. Therefore a piecewise constant function q is in \hat{Y}_h^{WF} if and only if the DOFs (4.1a) are single-valued (cf. Remark 4.5). Likewise, if a piecewise linear polynomial v is single-valued at the DOFs (4.2), then the proof of Lemma 4.7 shows that the function is continuous, i.e., $v \in V_h^{\text{WF}}$. Conversely, Lemma 4.3 shows that the DOFs (4.2) are single-valued on $V_h^{\rm WF}$.

From Lemma 4.6, we see that a function $q \in Y_h^{WF}$ is uniquely determined by

$$\int_{e} \llbracket q \rrbracket_{e} \qquad \forall e \in \Delta_{1}^{I}(F^{\text{CT}}) \backslash \{e_{F}\}, \ \forall F \in \Delta_{2}(\mathcal{T}_{h}),$$

$$\int_{T} qp \qquad \forall p \in \mathcal{P}_{0}(T^{\text{A}}), \forall T \in \mathcal{T}_{h},$$
(4.3a)

$$\int_{\mathbb{T}} qp \qquad \forall p \in \mathcal{P}_0(T^{\mathcal{A}}), \forall T \in \mathcal{T}_h, \tag{4.3b}$$

and a function $q \in \hat{Y}_h^{\text{WF}}$ is determined by (4.3) but with (4.3a) restricted to interior faces. Likewise, Lemma 4.7 shows that a function $\mathbf{v} \in V_h^{\text{WF}}$ is uniquely determined by the values

$$\mathbf{v}(a) \qquad \forall a \in \Delta_0(\mathcal{T}_h), \tag{4.4a}$$

$$\int_{F} (\boldsymbol{v} \cdot \boldsymbol{n}_{F}) \qquad \forall F \in \Delta_{2}(\mathcal{T}_{h}), \tag{4.4b}$$

$$\int_{\mathbb{R}} [[\operatorname{div} \mathbf{v}]]_e \qquad \forall e \in \Delta_1^I(F^{\text{CT}}) \setminus \{e_F\}, \ \forall F \in \Delta_2(\mathcal{T}_h), \tag{4.4c}$$

$$\int_{T} (\operatorname{div} \boldsymbol{v}) p \qquad \forall p \in \mathring{\mathcal{V}}_{0}(T), \forall T \in \mathcal{T}_{h}, \tag{4.4d}$$

and a function $v \in \mathring{V}_h^{\text{WF}}$ is uniquely determined by (4.4) but with (4.4a) and (4.4b)–(4.4c) restricted to interior vertices and interior faces, respectively.

Remark 4.9. Because dim $\mathcal{P}_0(T^A) = 4$, the DOFs show dim $\hat{Y}_h^{\mathrm{WF}} = 4|\mathcal{T}_h| + 2|\mathcal{F}_h^I|$, where $|\mathcal{F}_h^I|$ denotes the number of interior faces in \mathcal{T}_h . Likewise, dim $\mathring{V}_h^{\mathrm{WF}} = 3(|\mathcal{V}_h^I| + |\mathcal{F}_h^I| + |\mathcal{T}_h|)$, where $|\mathcal{V}_h^I|$ denotes the number of interior vertices in \mathcal{T}_h . This dimension count agrees with three times the number of interior vertices in $\mathcal{T}_h^{\mathrm{WF}}$.

We will need the following estimate to prove inf-sup stability.

Proposition 4.10. Let $v \in V_h^{WF}$ and $T \in \mathcal{T}_h$. For m = 0, 1, there holds

$$|\mathbf{v}|_{H^m(T)} \leq C h_T^{-1-2m} \Big(h_T^4 \sum_{a \in \Delta_0(T)} |\mathbf{v}(a)|^2 + \sum_{F \in \Delta_2(T)} \Big| \int_F \mathbf{v} \cdot \mathbf{n}_F \Big|^2 + h_T^3 \|\text{div } \mathbf{v}\|_{L^2(T)}^2 \Big).$$

Proof. Let \hat{T} be the reference tetrahedron, and let $F_T: \hat{T} \to T$ be an affine bijection with $F_T(\hat{x}) = A_T\hat{x} + b_T$ with $A_T \in \mathbb{R}^{3 \times 3}$ and $b_T \in \mathbb{R}^3$. We define $\hat{v}: \hat{T} \to \mathbb{R}^3$ via the Piola transform

$$\mathbf{v}(x) = \frac{A_T \hat{\mathbf{v}}(\hat{x})}{\det(A_T)}, \qquad x = F_T(\hat{x}).$$

Let \hat{T}^{WF} be the split of \hat{T} induced by T^{WF} and the mapping F_T^{-1} , i.e.,

$$\hat{T}^{WF} = \{ F_T^{-1}(K) : K \in T^{WF} \}.$$

Then \hat{v} is a continuous piecewise linear polynomial with respect to \hat{T}^{WF} , and therefore by equivalence of norms, and Lemma 4.7,

$$\begin{split} |\hat{\pmb{v}}|_{H^m(\hat{T})}^2 &\leq C \Big(\sum_{\hat{a} \in \Delta_0(\hat{T})} |\hat{\pmb{v}}(\hat{a})|^2 + \sum_{\hat{F} \in \Delta_2(\hat{T})} \Big| \int_{\hat{F}} \hat{\pmb{v}} \cdot \hat{\pmb{n}}_{\hat{F}} \Big|^2 \\ &+ \sum_{\hat{F} \in \Delta_2(\hat{T})} \sum_{\hat{e} \in \Delta_1^I(\hat{F}^{\text{CT}}) \backslash \{\hat{e}_{\hat{F}}\}} \Big| \int_{\hat{e}} \Big[\widehat{\text{div}} \, \hat{\pmb{v}} \Big]_{\hat{e}} \Big|^2 + \sup_{\hat{p} \in \mathring{V}_0(\hat{T}) \atop \|\hat{p}\|_{L^2(\hat{T})} = 1} \Big| \int_{\hat{T}} (\widehat{\text{div}} \, \hat{\pmb{v}}) \hat{p} \Big|^2 \Big), \end{split}$$

where $\mathring{V}_0(\hat{T}) = \mathcal{P}_0(\hat{T}^A) \cap L_0^2(\hat{T})$, and \hat{T}^A is the split of \hat{T} induced by T^A and the mapping F_T^{-1} . By well-known properties of the Piola transform, we have

$$\operatorname{div} \boldsymbol{v}(x) = \frac{1}{\det(A_T)} \widehat{\operatorname{div}} \, \widehat{\boldsymbol{v}}(\hat{x}), \qquad \int_F \boldsymbol{v} \cdot \boldsymbol{n}_F = \int_{\hat{F}} \widehat{\boldsymbol{v}} \cdot \widehat{\boldsymbol{n}}_{\hat{F}}.$$

Thus, we have

$$\begin{split} |\hat{\pmb{v}}|_{H^{m}(\hat{T})}^{2} & \leq C \Big(\sum_{a \in \Delta_{0}(T)} |\det(A_{T}) A_{T}^{-1} \pmb{v}(a)|^{2} + \sum_{F \in \Delta_{2}(T)} \left| \int_{F} \pmb{v} \cdot \pmb{n}_{F} \right|^{2} \\ & + |\det(A_{T})|^{2} \sum_{F \in \Delta_{2}(T)} \sum_{e \in \Delta_{1}(F) \setminus \{e_{F}\}} \left| \frac{|\hat{e}|}{|e|} \int_{e} [\![\operatorname{div} \pmb{v}]\!]_{e} \right|^{2} + \sup_{\substack{\hat{p} \in \mathring{V}_{0}(\hat{T}) \\ \|\hat{p}\|_{L^{2}(\hat{T})} = 1}} \left| \int_{\hat{T}} (\widehat{\operatorname{div}} \hat{\pmb{v}}) \hat{p} \right|^{2} \Big). \end{split}$$

Next, for $\hat{p} \in \mathring{\mathcal{V}}_0(\hat{T})$ with $\|\hat{p}\|_{L^2(\hat{T})} = 1$, let $p: T \to \mathbb{R}$ be given by $p(x) = \hat{p}(\hat{x})$. Then $p \in \mathring{\mathcal{V}}_0(T)$, $||p||_{L^2(T)} = \sqrt{6|T|}$, and

$$\int_{\hat{T}} (\widehat{\operatorname{div}}\,\hat{\boldsymbol{v}}) \hat{p} = \int_{T} (\operatorname{div}\,\boldsymbol{v}) p.$$

We conclude

$$\begin{split} \sup_{\hat{p} \in \mathring{V}_{0}(\hat{T})} \bigg| \int_{\hat{T}} (\widehat{\operatorname{div}} \, \hat{\pmb{v}}) \hat{p} \bigg|^{2} &\leq \sup_{\substack{p \in \mathring{V}_{0}(T) \\ \|\hat{p}\|_{L^{2}(T)} = \sqrt{6|T|}}} \bigg| \int_{T} (\operatorname{div} \, \pmb{v}) p \bigg|^{2} \\ &\leq \sup_{\substack{p \in \mathring{V}_{0}(T) \\ \|p\|_{L^{2}(T)} = \sqrt{6|T|}}} \|\operatorname{div} \, \pmb{v}\|_{L^{2}(T)}^{2} \|p\|_{L^{2}(T)}^{2} = 6|T| \|\operatorname{div} \, \pmb{v}\|_{L^{2}(T)}^{2} \leq Ch_{T}^{3} \|\operatorname{div} \, \pmb{v}\|_{L^{2}(T)}^{2}. \end{split}$$

Finally, we use $||A_T^{-1}|| \le Ch_T^{-1}$ and $|\det(A_T)| = 6|T| \le Ch_T^3$ to get

$$\begin{split} \left| \hat{\boldsymbol{v}} \right|^2_{H^m(\hat{T})} & \leq C \left(h_T^4 \sum_{a \in \Delta_0(T)} |\boldsymbol{v}(a)|^2 + \sum_{F \in \Delta_2(T)} \left| \int_F \boldsymbol{v} \cdot \boldsymbol{n}_F \right|^2 \\ & + h_T^4 \sum_{F \in \Delta_2(T)} \sum_{e \in \Delta_1^I(F^{\text{CT}}) \setminus \{e_F\}} \left| \int_e \left[\operatorname{div} \boldsymbol{v} \right] \right|_e \right|^2 + h_T^3 \left\| \operatorname{div} \boldsymbol{v} \right\|_{L^2(T)}^2 \right), \end{split}$$

and therefore

$$\begin{split} \| \boldsymbol{v} \|_{H^{m}(\hat{T})}^{2} & \leq C h_{T}^{-1-2m} | \hat{\boldsymbol{v}} \|_{H^{m}(\hat{T})}^{2} \leq C h_{T}^{-1-2m} \left(h_{T}^{4} \sum_{a \in \Delta_{0}(T)} |\boldsymbol{v}(a)|^{2} + \sum_{F \in \Delta_{2}(T)} \left| \int_{F} \boldsymbol{v} \cdot \boldsymbol{n}_{F} \right|^{2} \\ & + h_{T}^{4} \sum_{F \in \Delta_{2}(T)} \sum_{e \in \Delta_{1}(F) \setminus \{e_{F}\}} \left| \int_{e} [\![\operatorname{div} \boldsymbol{v}]\!]_{e} \right|^{2} + h_{T}^{3} \|\operatorname{div} \boldsymbol{v}\|_{L^{2}(T)}^{2} \right) \\ & \leq C h_{T}^{-1-2m} \left(h_{T}^{4} \sum_{a \in \Delta_{0}(T)} |\boldsymbol{v}(a)|^{2} + \sum_{F \in \Delta_{2}(T)} \left| \int_{F} \boldsymbol{v} \cdot \boldsymbol{n}_{F} \right|^{2} + h_{T}^{3} \|\operatorname{div} \boldsymbol{v}\|_{L^{2}(T)}^{2} \right), \end{split}$$

where the last inequality comes from standard trace and inverse inequalities. \Box

Theorem 4.11. The pair $\mathring{V}_{h}^{\text{WF}} \times \mathring{Y}_{h}^{\text{WF}}$ is inf–sup stable.

Proof. Fix $q \in \mathring{Y}_h^{\mathrm{WF}}$, and let $\mathbf{w} \in \mathring{\boldsymbol{H}}^1(\Omega)$ satisfy div $\mathbf{w} = q$ and $\|\nabla \mathbf{w}\|_{L^2(\Omega)} \le C \|q\|_{L^2(\Omega)}$. Let $\mathbf{w}_h \in \mathring{\mathcal{P}}_1(\mathfrak{T}_h)$ be the Scott-Zhang interpolant of \mathbf{w} with respect to \mathfrak{T}_h [19]. Define $\mathbf{v} \in V_h^{\mathrm{WF}}$ such that (cf. (4.4))

$$\begin{aligned} & \boldsymbol{v}(a) = \boldsymbol{w}_h(a) & \forall a \in \Delta_0(\mathfrak{T}_h), \\ & \int_F (\boldsymbol{v} \cdot \boldsymbol{n}_F) = \int_F (\boldsymbol{w} \cdot \boldsymbol{n}_F) & \forall F \in \Delta_2(\mathfrak{T}_h), \\ & \int_e [\![\operatorname{div} \boldsymbol{v}]\!]_e = \int_e [\![q]\!]_e & \forall e \in \Delta_1^I(F^{\operatorname{CT}}) \backslash \{e_F\}, \ \forall F \in \Delta_2(\mathfrak{T}_h), \\ & \int_T (\operatorname{div} \boldsymbol{v}) p = \int_T q p & \forall p \in \mathring{\mathcal{V}}_0(T), \forall T \in \mathfrak{T}_h. \end{aligned}$$

Noting $(\operatorname{div} \boldsymbol{v} - q) \in Y_h^{\operatorname{WF}}$ (cf. Lemma 4.3) and using Lemma 4.6 we conclude that $\operatorname{div} \boldsymbol{v} = q$. The proof of Lemma 4.7 shows $\boldsymbol{v} \in \mathring{\boldsymbol{V}}_h^{WF}$ since $\boldsymbol{w}, \boldsymbol{w}_h \in \mathring{\boldsymbol{H}}^1(\Omega)$. We apply Proposition 4.10 to $(\boldsymbol{v} - \boldsymbol{w}_h)$ with m = 1:

$$\|\nabla(\boldsymbol{v} - \boldsymbol{w}_h)\|_{L^2(T)}^2 \le Ch_T^{-3} \left(h_T^4 \sum_{a \in \Delta_0(T)} |(\boldsymbol{v} - \boldsymbol{w}_h)(a)|^2 + \sum_{F \in \Delta_2(T)} \left| \int_F (\boldsymbol{v} - \boldsymbol{w}_h) \cdot \boldsymbol{n}_F \right|^2 + h_T^3 \|\operatorname{div}(\boldsymbol{v} - \boldsymbol{w}_h)\|_{L^2(T)}^2 \right)$$

$$= Ch_{T}^{-3} \left(\sum_{F \in \Delta_{2}(T)} \left| \int_{F} (\boldsymbol{w} - \boldsymbol{w}_{h}) \cdot \boldsymbol{n}_{F} \right|^{2} + h_{T}^{3} \|q - \operatorname{div} \boldsymbol{w}_{h}\|_{L^{2}(T)}^{2} \right)$$

$$\leq Ch_{T}^{-3} \left(h_{T}^{2} \sum_{F \in \Delta_{2}(T)} \|\boldsymbol{w} - \boldsymbol{w}_{h}\|_{L^{2}(F)}^{2} + h_{T}^{3} \|q - \operatorname{div} \boldsymbol{w}_{h}\|_{L^{2}(T)}^{2} \right)$$

$$\leq C \left(\|q\|_{L^{2}(T)}^{2} + \|\nabla \boldsymbol{w}_{h}\|_{L^{2}(T)}^{2} + h_{T}^{-1} \|\boldsymbol{w} - \boldsymbol{w}_{h}\|_{L^{2}(\partial T)}^{2} \right)$$

$$\leq C \left(\|q\|_{L^{2}(T)}^{2} + h_{T}^{-2} \|\boldsymbol{w} - \boldsymbol{w}_{h}\|_{L^{2}(T)}^{2} + \|\nabla (\boldsymbol{w} - \boldsymbol{w}_{h})\|_{L^{2}(T)}^{2} + \|\nabla \boldsymbol{w}_{h}\|_{L^{2}(T)}^{2} \right) ,$$

where we used a standard trace inequality in the last inequality. We then sum over $T \in \mathcal{T}_h$ and apply stability and approximation properties of the Scott–Zhang interpolant to conclude $\|\nabla \boldsymbol{v}\|_{L^2(\Omega)} \leq C \|q\|_{L^2(\Omega)}$. \square

5. Implementation aspects for Powell–Sabin splits

The only tricky part to implement these finite elements is the pressure spaces since they have non-standard constraints in their definitions. In this section and the subsequent one, we give details to form the algebraic system for the Stokes problem.

5.1. A basis for \hat{Y}_{h}^{PS} and the construction of the algebraic system

Recall that the space \hat{Y}_h^{PS} consists of piecewise constant functions satisfying a weak continuity property at vertices. Clearly, this is a non-standard space, and in particular the space is not explicitly found in current finite element software packages. Nonetheless, in this section, we identify a basis of the space \hat{Y}_h^{PS} , and as a byproduct show that the weak continuity property $\theta_z(q) = 0$ can be imposed purely at the algebraic level.

As a first step, we note that, by definition of the Powell–Sabin triangulation,

$$\mathfrak{I}_h^{\mathrm{PS}} = \{ K_z^{(j)} : K_z^{(j)} \in \mathfrak{I}_z, \ z \in \mathcal{S}_h \}.$$

With this (implicit) labeling of the triangles in \mathfrak{T}_h^{PS} , we can write the canonical basis of $\mathfrak{P}_0(\mathfrak{T}_h^{PS})$ as the set $\{\varphi_z^{(j)}\}\subset \mathcal{P}_0(\mathfrak{T}_h^{\mathrm{PS}})$ with

$$\varphi_z^{(j)}|_{\kappa^{(i)}} = \delta_{v,z}\delta_{i,j} \qquad \forall z, v \in S_h, \ i = 1, \dots, n_v, \ j = 1, \dots, n_z.$$

The next proposition shows that a basis of \hat{Y}_h^{PS} is easily extracted from the basis of $\mathcal{P}_0(\mathcal{T}_h^{PS})$ (see Fig. 4).

Proposition 5.1. For each $z \in S_h$ and $j \in \{2, ..., n_z\}$, define

$$\psi_z^{(j)} = \varphi_z^{(j)} + (-1)^j \varphi_z^{(1)}.$$

Then $\{\psi_z^{(j)}: z \in \mathbb{S}_h, j = 2, ..., n_z\}$ forms a basis of \hat{Y}_h^{PS} .

Proof. Note that the number of functions $\{\psi_z^{(j)}\}$ given is $\sum_{z\in\mathcal{S}_h}(n_z-1)$, and

$$\dim \hat{Y}_h^{PS} = \dim \mathcal{P}_0(\mathcal{T}_h^{PS}) - |\mathcal{S}_h| = \sum_{z \in \mathcal{S}_h} n_z - |\mathcal{S}_h| = \sum_{z \in \mathcal{S}_h} (n_z - 1).$$

Because $\psi_z^{(j)} \in \hat{Y}_h^{PS}$, and they are clearly linear independent, we conclude that $\{\psi_z^{(j)}\}$ form a basis of \hat{Y}_h^{PS} . \square

We now explain how Proposition 5.1 provides a simple way to construct the stiffness matrix for the Stokes problem using the $\mathring{V}_h^{\rm PS} \times \mathring{Y}_h^{\rm PS}$ pair. To explain the procedure, we require some notation. Let A be the matrix associated with the bilinear form

$$(\boldsymbol{v}, \boldsymbol{w}) \to \int_{\Omega} v \nabla \boldsymbol{v} : \nabla \boldsymbol{w} \quad \text{over } \boldsymbol{v}, \boldsymbol{w} \in \mathring{\boldsymbol{V}}_{h}^{\text{PS}},$$

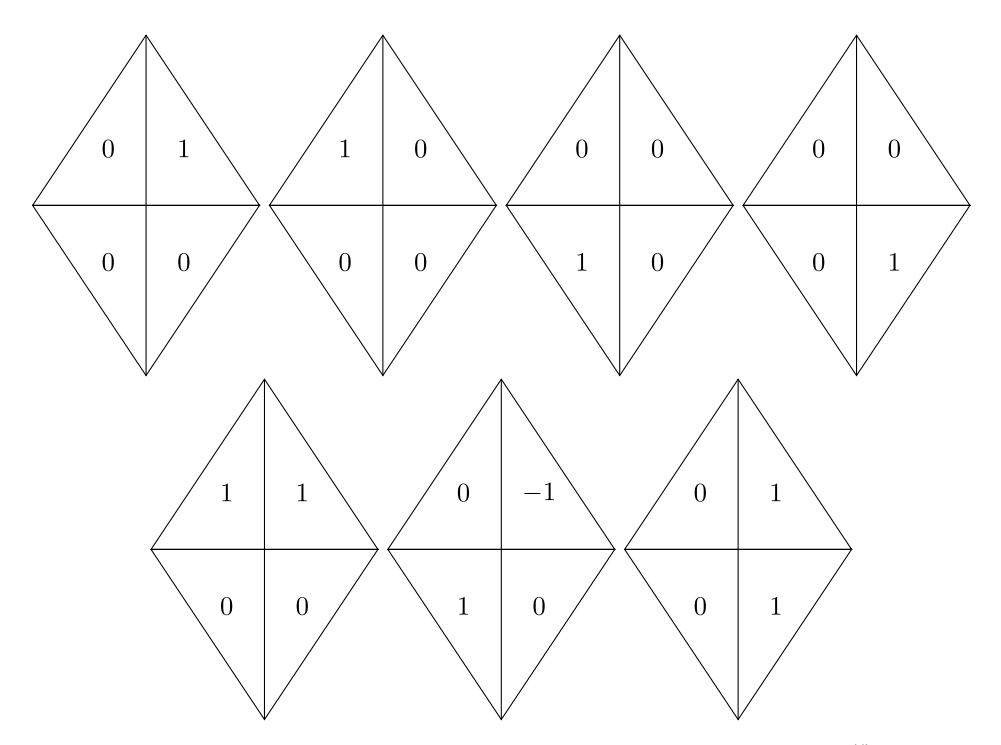


Fig. 4. Local mesh \mathcal{T}_z with $z \in \mathcal{S}_h^I$. Top row: Values of canonical basis functions of piecewise constants $\{\varphi_z^{(j)}\}_{j=1}^{n_z}$. Bottom row: Values of basis functions of piecewise constants with weak continuity constraint $\{\psi_z^{(j)}\}_{j=2}^{n_z}$.

and let \tilde{B} is the matrix associated with the bilinear form

$$(\boldsymbol{v},q) \to -\int_{\Omega} (\operatorname{div} \boldsymbol{v}) q \quad \text{over } \boldsymbol{v} \in \mathring{\boldsymbol{V}}_{h}^{\operatorname{PS}}, \ q \in \mathcal{P}_{0}(\mathfrak{T}_{h}^{\operatorname{PS}}).$$

The stiffness matrix for the Stokes problem based on the (unstable) $\mathring{\boldsymbol{V}}_h^{\mathrm{PS}} \times \mathcal{P}_0(\mathfrak{T}_h^{\mathrm{PS}})$ pair is given by

$$\begin{pmatrix} A & \tilde{B} \\ \tilde{B}^{\dagger} & 0 \end{pmatrix}$$
.

We emphasize that this system can be easily constructed using standard finite element software packages. Let $\{\phi^{(i)}\}_{k=1}^N$ denote a basis of \mathring{V}_h^{PS} with $N=\dim\mathring{V}_h^{PS}$ so that

$$A_{i,j} = \nu \int_{\Omega} \nabla \boldsymbol{\phi}^{(j)} : \nabla \boldsymbol{\phi}^{(i)} \, dx.$$

Let $M=\dim \mathcal{P}_0(\mathfrak{T}_h^{\mathrm{PS}})$, the number of triangles in $\mathfrak{T}_h^{\mathrm{PS}}$, and introduce the local-to-global label mapping $\sigma: \mathbb{S} \times \{1,\ldots,n_z\} \to \{1,2,\ldots,M\}$ such that

$$\tilde{B}_{i,\sigma(z,j)} = -\int_{\Omega} (\operatorname{div} \boldsymbol{\phi}^{(i)}) \varphi_z^{(j)}.$$

Then by Proposition 5.1, we have for $z \in S_h$ and $j = 2, ..., n_z$,

$$-\int_{\Omega} (\operatorname{div} \boldsymbol{\phi}^{(i)}) \psi_{z}^{(j)} = -\int_{\Omega} (\operatorname{div} \boldsymbol{\phi}^{(i)}) \varphi_{z}^{(j)} - (-1)^{j} \int_{\Omega} (\operatorname{div} \boldsymbol{\phi}^{(i)}) \varphi_{z}^{(1)}$$
$$= \tilde{B}_{i,\sigma(z,j)} + (-1)^{j} \tilde{B}_{i,\sigma(z,1)}.$$

This identity leads to the following algorithm.

Algorithm

- 1. Construct Powell–Sabin triangulation \mathfrak{T}_h^{PS} 2. Construct $\tilde{B} \in \mathbb{R}^{N \times M}$ based on the $\mathring{V}_h^{PS} \times \mathcal{P}_0(\mathfrak{T}_h^{PS})$ pair.
- 3. Set $B = \tilde{B}$.
- 4. For each $z \in S_h$ and for each $i \in \{2, \dots, n_z\}$, do the elementary column operation

$$B_{:,\sigma(z,j)} = B_{:,\sigma(z,j)} + (-1)^j B_{:,\sigma(z,1)}.$$

5. Delete column $B_{:,\sigma(z,1)}$ for each $z \in S_h$.

The stiffness matrix for the Stokes problem based on the $\mathring{V}_h^{PS} \times \hat{Y}_h^{PS}$ pair is then given by

$$\begin{pmatrix} A & B \\ B^{\mathsf{T}} & 0 \end{pmatrix}. \tag{5.1}$$

Remark 5.2. In the numerical experiments below, we further delete a single arbitrary row and column of the matrix B in (5.1). This modification mods out the global constant function in the space \hat{Y}_h^{PS} , and Theorem 3.4 implies that the reduced saddle point problem is invertible. A simple post-processing step is then performed on the discrete pressure solution to impose the zero mean-value constraint. Alternatively, the mean-value constraint can be imposed via a standard Lagrange multiplier.

6. Implementation aspects for Worsey-Farin splits

6.1. A basis for \hat{Y}_h^{WF} and the construction of the algebraic system

Notice that the collection of local triangulations \mathcal{T}_e (with $e \in \mathcal{E}_h^{\mathcal{S}}$) do not form a disjoint partition of the global triangulation $\mathcal{T}_h^{\mathrm{WF}}$. In particular, there exists $K \in \mathcal{T}_h^{\mathrm{WF}}$ such that $K \in \mathcal{T}_e$ and $K \in \mathcal{T}_s$ with $e, s \in \mathcal{E}_h^{\mathcal{S}}$ and $e \neq s$. As a result, the methodology used in the previous section for Powell-Sabin meshes is not directly applicable.

Instead, we consider a geometric decomposition of the mesh based on the face split points in $\mathfrak{T}_h^{\text{WF}}$. To this end, we denote by S_h^I and S_h^B the sets of interior and boundary face split points, respectively, and set $S_h = S_h^I \cup S_h^B$. For $z \in S_h$, let $\mathcal{T}_z := \{K_z^{(1)}, \ldots, K_z^{(n_z)}\}$ denote the set of tetrahedra in $\mathcal{T}_h^{\text{WF}}$ that have z as a vertex (cf. Fig. 5). Here, $n_z = 6$ if z is an interior vertex, and $n_z = 3$ if z is a boundary vertex. For an interior face split point z, we assume the simplices in T_z are labeled such that

$$K_z^{(1)}, K_z^{(2)}, K_z^{(3)} \subset T^{(1)}, \qquad K_z^{(4)}, K_z^{(5)}, K_z^{(6)} \subset T^{(2)}$$

for some $T^{(1)}$, $T^{(2)} \in \mathcal{T}_h$, and that $K_z^{(j)}$ and $K_z^{(j+3)}$ share a common face for $j \in \{1, 2, 3\}$. For a boundary split point z, the set $\mathcal{T}_z = \{K_z^{(1)}, K_z^{(2)}, K_z^{(3)}\}$ is labeled arbitrarily.

We clearly have

$$\mathcal{T}_h^{\text{WF}} = \{ K_z^{(j)} : z \in \mathcal{S}_h, j = 1, \dots, n_z \}, \tag{6.1}$$

and the map $(z, j) \to K_z^{(j)}$ is injective. Furthermore, each local partition \mathfrak{T}_z contains three singular edges.

Proposition 6.1. There holds

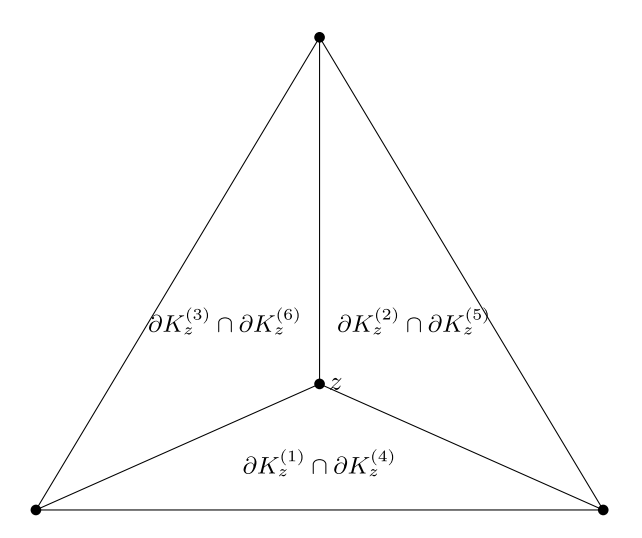
$$\dim \hat{Y}_h^{\text{WF}} = 4|\mathcal{S}_h^I| + |\mathcal{S}_h^B|.$$

Proof. Recall from Remark 4.9 that

$$\dim \hat{Y}_h^{\text{WF}} = 4|\mathcal{T}_h| + 2|\mathcal{F}_h^I|,$$

where $|\mathcal{F}_h^I|$ is the number of interior faces in \mathcal{T}_h . From (6.1), we have

$$12|\mathcal{T}_h| = |\mathcal{T}_h^{WF}| = 6|\mathcal{S}_h^I| + 3|\mathcal{S}_h^B|,$$



Computer Methods in Applied Mechanics and Engineering 390 (2022) 114444

Fig. 5. Cross-section of the Clough-Tocher refinement of an interior face $F = \partial T^{(1)} \cap \partial T^{(2)}$ with face split point z.

and by construction of the Worsey-Farin split, there holds

$$|\mathcal{F}_h^I| = |\mathcal{S}_h^I|.$$

Therefore,

$$\dim \hat{Y}_h^{\text{WF}} = 4|\mathcal{T}_h| + 2|\mathcal{F}_h^I| = \frac{1}{3} \left(6|\mathcal{S}_h^I| + 3|\mathcal{S}_h^B| \right) + 2|\mathcal{S}_h^I| = 4|\mathcal{S}_h^I| + |\mathcal{S}_h^B|. \quad \Box$$

For an interior split point z, and for a piecewise constant function q on \mathfrak{T}_z , the three constraints $\theta_e(q) = 0$ read

$$q_1 - q_2 + q_5 - q_4 = 0,$$

$$q_2 - q_3 + q_6 - q_5 = 0$$

$$q_3 - q_1 + q_4 - q_6 = 0,$$

where $q_j = q|_{K_z^{(j)}}$ We write this as a 3 × 6 linear system

$$C\vec{q} := \begin{pmatrix} 1 & -1 & 0 & -1 & 1 & 0 \\ 0 & 1 & -1 & 0 & -1 & 1 \\ -1 & 0 & 1 & 1 & 0 & -1 \end{pmatrix} \begin{pmatrix} q_1 \\ q_2 \\ q_3 \\ q_4 \\ q_5 \\ q_6 \end{pmatrix} = 0.$$

We clearly see that this matrix has rank 2 (e.g., adding the first and third rows gets the negation of the second row). We find that the nullspace of C is given by

$$\operatorname{null}(C) = \operatorname{span} \left\{ \begin{pmatrix} 1\\1\\1\\0\\0\\0 \end{pmatrix}, \begin{pmatrix} 1\\0\\0\\1\\0\\0 \end{pmatrix}, \begin{pmatrix} 0\\1\\0\\0\\1\\0 \end{pmatrix}, \begin{pmatrix} -1\\-1\\0\\0\\0\\1 \end{pmatrix} \right\}.$$

These four vectors implicitly give us a basis for \hat{Y}_h^{WF} . In particular, we have

Proposition 6.2. For $z \in \mathcal{S}_h$ and $j \in \{1, 2, ..., n_z\}$, let $\varphi_z^{(j)}$ be the piecewise constant function

$$\varphi_z^{(j)}|_{K_v^{(i)}} = \delta_{v,z}\delta_{i,j} \qquad \forall v, z \in \mathcal{S}_h, \ i = 1, \dots, n_v, \ j = 1, \dots, n_z.$$

For an interior face split point z, define

$$\psi_z^{(3)} = \varphi_z^{(3)} + \varphi_z^{(1)} + \varphi_z^{(2)},$$

$$\psi_z^{(4)} = \varphi_z^{(4)} + \varphi_z^{(1)},$$

$$\psi_z^{(5)} = \varphi_z^{(5)} + \varphi_z^{(2)},$$

$$\psi_z^{(6)} = \varphi_z^{(6)} - \varphi_z^{(1)} - \varphi_z^{(2)}.$$

For a boundary face split point z, define

$$\psi_z^{(3)} = \varphi_z^{(3)} + \varphi_z^{(1)} + \varphi_z^{(2)}.$$

Then $\{\psi_z^{(j)}\}$ is a basis of \hat{Y}_h^{WF} .

Proof. The proof essentially follows from the same arguments as Proposition 5.1, noting that the number of given $\psi_{z}^{(j)}$ is

$$4|S_h^I| + |S_h^B| = \dim \hat{Y}_h^{WF}$$

by Proposition 6.1. \square

As in the two-dimensional case, Proposition 6.2 gives an algorithm to construct the stiffness matrix for the Stokes problem using the $\mathring{\boldsymbol{V}}_h^{\mathrm{WF}} \times \hat{Y}_h^{\mathrm{WF}}$ pair. First, we construct the stiffness matrix based on the $\mathring{\boldsymbol{V}}_h^{\mathrm{WF}} \times \mathcal{P}_0(\mathcal{T}_h^{\mathrm{WF}})$ pair:

$$\begin{pmatrix} A & \tilde{B} \\ \tilde{B}^{\intercal} & 0 \end{pmatrix},$$

and then perform elementary column operations on the \tilde{B} . Let $\{\phi^{(k)}\}_{k=1}^N$ denote a basis of $\mathring{V}_h^{\text{WF}}$ with $N=\dim\mathring{V}_h^{\text{WF}}$. Let $M=\dim\mathcal{P}_0(\mathfrak{T}_h^{\text{PS}})$, the number of tetrahedra in $\mathfrak{T}_h^{\text{WF}}$, and introduce the local-to-global label mapping $\sigma: \mathcal{S}_h \times \{1,\ldots,n_z\} \to \{1,2,\ldots,M\}$ such that

$$\tilde{B}_{k,\sigma(z,j)} = -\int_{\Omega} (\operatorname{div} \boldsymbol{\phi}^{(k)}) \varphi_z^{(j)}.$$

Algorithm 1

- 1. Construct Worsey–Farin triangulation \mathfrak{T}_h^{PS} 2. Construct $\tilde{B} \in \mathbb{R}^{N \times M}$ based on the $\mathring{V}_h^{WF} \times \mathfrak{P}_0(\mathfrak{T}_h^{WF})$ pair.
- 3. Set $B = \tilde{B}$
- 4. For each interior face split point $z \in S_h$ do the elementary column operations

$$\begin{split} B_{:,\sigma(z,3)} &= B_{:,\sigma(z,3)} + B_{:,\sigma(z,1)} + B_{:,\sigma(z,2)}, \\ B_{:,\sigma(z,4)} &= B_{:,\sigma(z,4)} + B_{:,\sigma(z,1)}, \\ B_{:,\sigma(z,5)} &= B_{:,\sigma(z,5)} + B_{:,\sigma(z,2)}, \\ B_{:,\sigma(z,6)} &= B_{:,\sigma(z,6)} - B_{:,\sigma(z,1)} - B_{:,\sigma(z,2)}. \end{split}$$

5. For each boundary face split point $z \in S_h$ do the elementary column operation

$$B_{:,\sigma(z,3)} = B_{:,\sigma(z,3)} + B_{:,\sigma(z,1)} + B_{:,\sigma(z,2)}$$

6. Delete columns $B_{:,\sigma(z,1)}$ and $B_{:,\sigma(z,2)}$ for each $z \in S_h$.

The stiffness matrix for the Stokes problem based on the $\mathring{V}_h^{\mathrm{WF}} \times \hat{Y}_h^{\mathrm{WF}}$ pair is then given by

$$\begin{pmatrix} A & B \\ B^{\mathsf{T}} & 0 \end{pmatrix}, \tag{6.2}$$

Remark 6.3. In the numerical experiments below, we further delete an arbitrary row and column of B to ensure the system (6.2) is invertible; cf. Remark 5.2.

Table	1											
Errors	and	rates	of	convergence	for	the	2D	example	(7.3)	with	$\nu =$	1.

h	$\ \boldsymbol{u}-\boldsymbol{u}_h\ _{L^2(\Omega)}$	Rate	$\ p-p_h\ _{L^2(\Omega)}$	Rate	$\ \nabla \cdot \boldsymbol{u}_h\ _{L^2(\Omega)}$	β
2^{-2}	1.70E-01	_	5.26E 00	_	2.70E-14	1.56E-01
2^{-3}	5.66E - 02	1.587	3.77E 00	0.480	6.65E-14	1.38E-01
2^{-4}	1.35E-02	2.068	1.68E 00	1.166	2.38E-13	1.07E - 01
2^{-5}	3.35E-03	2.011	8.28E-01	1.021	8.38E-12	1.06E-01
2^{-6}	8.77E-04	1.934	4.25E-01	0.962	4.05E-10	9.34E-02

Table 2 Errors and rates of convergence for the 2D example (7.3) with $\nu = 10^{-2}$.

h	$\ \boldsymbol{u}-\boldsymbol{u}_h\ _{L^2(\Omega)}$	Rate	$ p-p_h _{L^2(\Omega)}$	Rate	$\ \nabla \cdot \boldsymbol{u}_h\ _{L^2(\Omega)}$
2^{-2}	1.70E-01	_	1.02E-01	_	2.43E-14
2^{-3}	5.66E - 02	1.587	5.79E - 02	0.816	5.88E-14
2^{-4}	1.35E-02	2.068	2.76E - 02	1.069	2.36E-13
2^{-5}	3.35E-03	2.011	1.37E-02	1.010	8.39E-12
2^{-6}	8.77E - 04	1.934	6.96E - 03	0.977	4.05E-10

7. Numerical experiments

In this section, we perform some simple numerical experiments for the Stokes problem on Powell–Sabin and Worsey–Farin splits. We note standard theory shows that the velocity and pressure errors satisfy

$$|\boldsymbol{u} - \boldsymbol{u}_h|_{H^1(\Omega)} \le (1 + \beta^{-1}) \inf_{\boldsymbol{v}_h \in \mathring{\boldsymbol{V}}_h} |\boldsymbol{v}_h - \boldsymbol{u}|_{H^1(\Omega)},$$
 (7.1)

$$\|p - p_h\|_{L^2(\Omega)} \le \inf_{q \in \mathring{Y}_h} \|p - q\|_{L^2(\Omega)} + \frac{\nu}{\beta} |\boldsymbol{u} - \boldsymbol{u}_h|_{H^1(\Omega)}, \tag{7.2}$$

where either $\mathring{V}_h \times \mathring{Y}_h = \mathring{V}_h^{PS} \times \mathring{Y}_h^{PS}$ or $\mathring{V}_h \times \mathring{Y}_h = \mathring{V}_h^{WF} \times \mathring{Y}_h^{WF}$, $\nu > 0$ is the viscosity, and β is the inf–sup constant for the finite element pair $\mathring{V}_h \times \mathring{Y}_h$.

7.1. The Stokes pair on Powell-Sabin splits

We consider the example such that the data is taken to be $\Omega = (0, 1)^2$, and the source function is chosen such that the exact velocity and pressure solutions for (2.1) are given respectively as

$$\mathbf{u} = \begin{pmatrix} \pi \sin^2(\pi x_1) \sin(2\pi x_2) \\ -\pi \sin^2(\pi x_2) \sin(2\pi x_1) \end{pmatrix}, \quad p = \cos(\pi x_1) \cos(\pi x_2). \tag{7.3}$$

Let \mathcal{T}_h be a Delaunay triangulation of Ω and \mathcal{T}_h^{PS} the corresponding Powell–Sabin global triangulation.

The resulting errors, rates of convergence, and inf-sup constants are listed in Tables 1 and 2 for viscosities $\nu=1$ and $\nu=10^{-2}$, respectively. We compute the inf-sup constants by solving a Stokes eigenvalue problem [23]. The results show that the L^2 pressure error and the H^1 velocity error converge with linear rate, the discrete velocity solution (and error) are independent of the viscosity ν , and the pressure error improves for small viscosity. The experiments also show that the inf-sup constant does not deteriorate as the mesh is refined with $\beta\approx 0.1$. These results are in agreement with the theoretical estimates (7.1)–(7.2)

In Tables 3 and 4, we compute the right-hand side of (7.2) and (7.1), respectively, and compare the data with the computed errors $\|p - p_h\|_{L^2(\Omega)}$ and $|u - u_h|_{H^1(\Omega)}$. Again, the results are consistent with (7.1)–(7.2), and they suggest that the term $\frac{v}{\beta}|u - u_h|_{H^1(\Omega)}$ is the dominant term in the pressure error (7.2) for moderately sized viscosity values.

Table 3 Errors for the 2D example (7.3) with $\nu = 10^{-2}$ and the RHS of (7.2).

h	$\ p-p_h\ _{L^2(\Omega)}$	$ \boldsymbol{u}-\boldsymbol{u}_h _{H^1(\Omega)}$	β	$\inf\nolimits_{q \in \mathring{Y}_h^{\mathrm{PS}}} \ p - q \ _{L^2(\Omega)}$	RHS of (7.2)
2^{-2}	1.02E-01	3.77E 00	1.56E-01	6.08E-02	3.02E-01
2^{-3}	5.79E - 02	2.17E 00	1.38E-01	2.77E-02	1.84E-01
2^{-4}	2.76E - 02	1.07E 00	1.07E - 01	1.35E-02	1.13E-01
2^{-5}	1.37E-02	5.32E-01	1.06E-01	6.61E-03	5.67E-02
2^{-6}	6.96E - 03	2.72E-01	9.34E-02	3.28E-03	3.24E-02

Table 4 Errors for the 2D example (7.3) with $\nu = 10^{-2}$ and the RHS of (7.1).

h	$ \boldsymbol{u}-\boldsymbol{u}_h _{H^1(\Omega)}$	β	$\inf_{\boldsymbol{v}_h \in \boldsymbol{V}_h^{\mathrm{PS}}} \boldsymbol{v}_h - \boldsymbol{u} _{H^1(\Omega)}$	RHS of (7.1)
2^{-2}	3.77E 00	1.56E-01	3.08E 00	2.28E+01
2^{-3}	2.17E 00	1.38E-01	1.63E 00	1.34E+01
2^{-4}	1.07E 00	1.07E - 01	8.04E-01	8.31E 00
2^{-5}	5.32E-01	1.06E-01	4.06E-01	4.23E 00
2^{-6}	2.72E-01	9.34E-02	2.05E-01	2.39E 00

Table 5 Errors and rates of convergence for the 3D example (7.4) with $\nu = 1$.

h	$\ \boldsymbol{u}-\boldsymbol{u}_h\ _{L^2(\Omega)}$	Rate	$\ p-p_h\ _{L^2(\Omega)}$	Rate	$\ \nabla \cdot \boldsymbol{u}_h\ _{L^2(\Omega)}$	β
1/2	1.29E 00	_	9.81E 00	_	5.07E-14	1.31E-01
1/4	8.58E-01	0.588	19.4E 00	-0.98	5.20E-13	1.31E-01
1/8	3.93E-01	1.286	16.6E 00	0.414	2.68E-12	1.32E-01
1/16	1.32E-01	1.573	10.5E 00	0.667	4.10E-12	1.32E-01
1/32	3.69E - 02	1.839	5.75E 00	0.872	4.32E-12	1.32E-01
1/48	1.68E-02	1.941	3.93E 00	0.936	6.07E-12	1.32E-01

7.2. The Stokes pair on Worsey-Farin splits

We consider the example such that the data is taken to be $\Omega = (0, 1)^3$, and the source function is chosen such that the exact velocity and pressure solutions for (2.1) are given respectively as

$$\mathbf{u} = \begin{pmatrix} \pi \sin^2(\pi x_1) \sin(2\pi x_2) \\ -\pi \sin^2(\pi x_2) \sin(2\pi x_1) \\ 0 \end{pmatrix}, \quad p = \cos(\pi x_1) \cos(\pi x_2) \cos(\pi x_3).$$
 (7.4)

Let \mathcal{T}_h be a Delaunay triangulation of Ω and \mathcal{T}_h^{WF} be the corresponding Worsey–Farin global triangulation.

The resulting rates of convergence of the numerical experiments for viscosities $\nu=1$ and $\nu=10^{-3}$ are listed in Tables 5 and 6, respectively. We also state the computed inf-sup constant on these meshes, and the results show that it stays uniformly bounded from below with $\beta\approx 0.13$ on all meshes. The stated errors, especially those in Table 5, indicate that the rates of convergence are still in the preasymptotic regime. On the other hand, for small viscosity value $\nu=10^{-3}$, Table 6 shows that the pressure error converges with linear rate. This behavior suggests that $|\boldsymbol{u}-\boldsymbol{u}_h|_{H^1(\Omega)}$ is larger than $\inf_{q\in \mathring{V}_h^{\mathrm{WF}}}\|p-q\|_{L^2(\Omega)}$, in particular, $\frac{\nu}{\beta}|\boldsymbol{u}-\boldsymbol{u}_h|_{H^1(\Omega)}$ is the dominating term in the pressure error (7.2) for moderately large viscosity values.

To verify this claim, we explicitly compute the terms in the right-hand side of (7.2) with $\nu = 1$ and report the results in Table 7. The results show that indeed $|\mathbf{u} - \mathbf{u}_h|_{H^1(\Omega)}$ is the dominating term in the pressure error (7.2).

7.3. A numerical comparison with the Crouzeix–Raviart Stokes pair

In this subsection, we consider the Crouzeix-Raviart [24] (CR) Stokes pair, and compare it to PS and WF Stokes pairs.

Table 6				
Errors and rates of convergence	for the 3D	example	(7.4) with	$\nu = 10^{-3}$.

h	$\ \boldsymbol{u}-\boldsymbol{u}_h\ _{L^2(\Omega)}$	Rate	$\ p-p_h\ _{L^2(\Omega)}$	Rate	$\ \nabla \cdot \boldsymbol{u}_h\ _{L^2(\Omega)}$
1/2	1.29E 00	_	1.33E-01	_	1.28E-15
1/4	8.58E-01	0.588	6.97E - 02	0.932	3.43E-14
1/8	3.93E-01	1.286	3.70E - 02	0.911	3.22E-13
1/16	1.32E-01	1.574	1.91E-02	0.953	6.40E - 13
1/32	3.69E - 02	1.838	9.68E - 03	0.980	9.52E-13
1/48	9.63E-03	1.940	4.89E - 03	0.983	1.03E-12

Table 7 Errors for the 3D example (7.4) with $\nu = 1$ and the RHS of (7.2).

h	$ p-p_h _{L^2(\Omega)}$	$\frac{v}{\beta} \boldsymbol{u}-\boldsymbol{u}_h _{H^1(\Omega)}$	$\inf_{q\in\mathring{Y}_h^{\mathrm{WF}}}\ p-q\ _{L^2(\Omega)}$	RHS of (7.2)
1/2	9.81E 00	8.17E+01	5.00E-01	8.22E+01
1/4	19.4E 00	6.49E + 01	6.70E - 02	6.50E+01
1/6	18.7E 00	5.17E+01	4.43E-02	5.17E+01
1/8	16.6E 00	4.24E+01	3.30E-02	4.25E+01
1/10	14.6E 00	3.57E+01	2.63E-02	3.57E+01
1/12	13.0E 00	3.08E+01	2.19E-02	3.08E+01

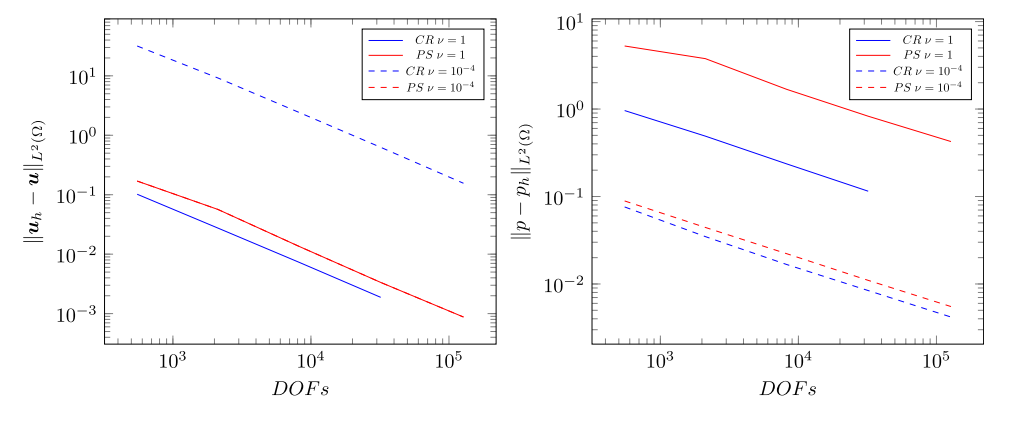


Fig. 6. PS and CR velocity (left) and pressure (right) errors with different viscosities.

7.3.1. CR pair vs. PS

We consider the example (7.3) on $\Omega = (0, 1)^2$. For the finite element pair, we consider the Crouzeix–Raviart (CR) element pair on the unrefined triangulation \mathfrak{T}_h .

The resulting errors and rates of convergence are compared with the Powell–Sabin pair in Fig. 6 for viscosities $\nu = 1$ and $\nu = 10^{-4}$. The mesh size updates in Fig. 6 are chosen so that the CR pair on mesh \mathcal{T}_h has a similar number of degrees of freedom as the PS pair on the corresponding mesh size updates of \mathcal{T}_h^{PS} in Tables 1 and 2 respectively.

For $\nu=1$, the L^2 velocity error magnitudes and (quadratic) convergence rates for the CR and PS pairs are comparable. The pressure L^2 error magnitudes for the CR pair are smaller than those for the PS element. Also, the convergence rates for the CR pair are more evident compared to the pressure convergence rates of the PS pair on coarse triangulations.

For $\nu = 10^{-4}$, the L^2 pressure error magnitudes and convergence rates for the CR and PS pairs are sufficiently close, similar to the $\nu = 1$ case. However, while the PS and CR velocity errors both converge quadratically, the velocity L^2 error magnitudes for the PS pair are significantly smaller than those for the CR pair. Unlike the CR pair, the velocity errors for PS pair are invariant with respect to the viscosity.

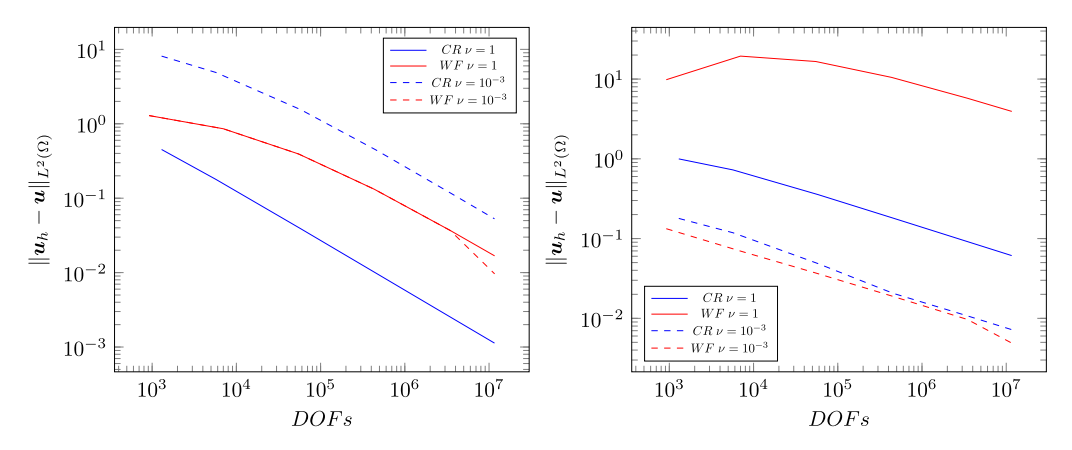


Fig. 7. WF vs. CR velocity and pressure errors with different viscosities.

7.3.2. CR pair vs. WF

We consider the example (7.4) on $\Omega = (0, 1)^3$. For the finite element pair, we consider the Crouzeix–Raviart element pair on the unrefined triangulation \mathcal{T}_h .

The resulting errors and rates of convergence are compared with the Worsey–Farin pair in Fig. 7 for viscosities $\nu = 1$ and $\nu = 10^{-3}$.

In the case of $\nu = 1$, and in contrast to the WF pair, we observe asymptotic convergence rates for the CR pair on relatively coarse meshes. The errors for both the velocity and pressure are smaller for the CR pair.

If we examine the case when $\nu = 10^{-3}$, we find that the errors for the pressure are comparable between the CR and WF pairs. The errors for the velocity are roughly one order of magnitude larger for the CR pair, when compared to those of the WF pair. Both methods exhibit similar convergence rates.

7.4. Iterated penalty method for $(\mathbf{P_1}, \mathbf{P_0})$ pair on Worsey–Farin splits

We consider the example such that the data is taken to be $\Omega = (0, 1)^3$, and the source function is chosen such that the exact velocity and pressure solutions for (2.1) are given respectively as

$$u(x, y, z) = \nabla \times \begin{pmatrix} 0 \\ g \\ g \end{pmatrix}, \quad p = \frac{1}{9} \frac{\partial^2 g}{\partial x \partial y},$$
 (7.5)

where

$$g = g(x, y, z) = 2^{12}(x - x^2)^2(y - y^2)^2(z - z^2)^2.$$

Similar to the previous section, we let \mathcal{T}_h be a Delaunay triangulation of Ω and $\mathcal{T}_h^{\text{WF}}$ be the corresponding Worsey–Farin global triangulation.

The iterated penalty method [25] applied to the Stokes equations with $\mathring{V}_h = \mathring{V}_h^{\text{WF}}$ reads: Let $\boldsymbol{u}_h^0 = \boldsymbol{0}$ and $\rho, \gamma > 0$ be parameters. For $n \ge 1$, \boldsymbol{u}_h^n is recursively defined to be the solution to the variational formulation

$$\nu(\nabla \boldsymbol{u}_{h}^{n}, \nabla \boldsymbol{v}) + \gamma(\nabla \cdot \boldsymbol{v}, \nabla \cdot \boldsymbol{u}_{h}^{n}) = (\boldsymbol{f}, \boldsymbol{v}) - (\sum_{i=0}^{n-1} \rho \nabla \cdot \boldsymbol{u}_{h}^{i}, \nabla \cdot \boldsymbol{v}), \quad \forall \boldsymbol{v} \in \mathring{\boldsymbol{V}}_{h}^{\text{WF}}.$$
(7.6)

It is shown in [25] that $\lim_{n\to\infty} \boldsymbol{u}_h^n = \boldsymbol{u}_h$ and $\lim_{n\to\infty} \sum_{i=0}^n \rho \nabla \cdot \boldsymbol{u}_h^i = p_h$. Also, [25] suggests to use $\|\nabla \cdot \boldsymbol{u}_h^n\|_{L^2(\Omega)}$ as a stopping criterion since the difference error between \boldsymbol{u}_h^n , \boldsymbol{u}_h is given by

$$\|\boldsymbol{u}_{h}^{n} - \boldsymbol{u}_{h}\|_{L^{2}(\Omega)} \leq C \|\nabla \cdot \boldsymbol{u}_{h}^{n}\|_{L^{2}(\Omega)}.$$

The resulting rates of convergence of the numerical experiment are listed in Table 8. The errors $\|\boldsymbol{u}-\boldsymbol{u}_h^n\|_{L^2(\Omega)}$ and $\|p-p_h^n\|_{L^2(\Omega)}$ are computed with $\|\nabla\cdot\boldsymbol{u}_h^n\|_{L^2(\Omega)}\leq 10^{-7}$ and $\gamma=\rho=100$.

Table 8 Errors and rates of convergence for example (7.5) with v = 1.

h	$\ \boldsymbol{u}-\boldsymbol{u}_h^n\ _{L^2(\Omega)}$	Rate	$ \boldsymbol{u}-\boldsymbol{u}_h^n _{H^1(\Omega)}$	Rate	$\ p-p_h^n\ _{L^2(\Omega)}$	Rate
1/4	1.11768	_	11.55063	_	25.32256	_
1/8	0.48896	1.19273	7.53829	0.61566	22.35349	0.17992
1/16	0.15482	1.65908	4.15598	0.85905	13.67635	0.70882
1/32	0.04176	1.89040	2.13224	0.96282	7.24129	0.91736
1/48	0.01881	1.96680	1.42643	0.99145	4.88909	0.96875

Table 9 Time comparison between (IPM) and Algorithm 1 for example (7.5) with $\nu=1$.

h	(IPM)	Algorithm 1
1/4	5.08E+00	3.35E+00
1/8	1.68E+01	2.93E+01
1/16	4.80E + 02	2.60E + 02
1/32	2.39E+03	9.37E + 02
1/48	7.31E+03	6.45E+03

In Table 9 we provide a time comparison between the (IPM) and the method described in Algorithm 1. All of the timings were done on a machine with a single 3.60 GHz Intel Core i9-9900K processor with 128 GB of 2400 MHz DDR4 memory.

For the iterated penalty method, we select $\gamma = \rho = 100$ and terminate iterations once $\|\nabla \cdot \boldsymbol{u}_h^n\|_{L^2(\Omega)} \le 10^{-7}$. At each iteration of IPM, Eq. (7.6) must be resolved. In our work, this vector Poisson problem type problem is solved via a conjugate gradient method with an algebraic multigrid (AMG) preconditioner. It is well known that optimal multigrid methods can be designed for this class of problems [26].

For Algorithm 1, we instead work with the full discretization matrix (6.2), which results in a symmetric indefinite linear system. To efficiently solve this saddle point problem, a block preconditioned Krylov subspace method is used [27]. In particular, we precondition the stiffness matrix (6.2) by the block diagonal matrix

$$\begin{pmatrix} A & 0 \\ 0 & S \end{pmatrix}$$
,

where $S = B^{\mathsf{T}}A^{-1}B$ is the Schur complement, and the flexible GMRES method as an outer iteration. The solver is terminated once the Euclidean norm of the residual is less than or equal to 10^{-8} . For simplicity, the inner preconditioners are as follows: we use a preconditioner to A for approximating A^{-1} , and the Schur complement is approximated as $S \approx B^{\mathsf{T}} \mathrm{diag}(A^{-1})B$. It should be noted that this is not the only choice for block-type preconditioning of the Stokes problem (e.g., see [28]); however, our numerical experiments indicate that we can repurpose existing preconditioners to efficiently solve linear systems that arise from the proposed finite element discretization.

From Table 9, it is evident that for a fixed mesh spacing, the total run times for both methods are competitive, with the IPM technique being slightly slower for larger meshes. We find that in the case of the linear Stokes problem, by utilizing preexisting preconditioners, both approaches provide similar accuracy and time to solution metrics.

To obtain a Reynolds robust, optimally scaling preconditioner, special multigrid techniques may have to be investigated [29,30].

Declaration of competing interest

The authors declare that they have no known competing financial interests or personal relationships that could have appeared to influence the work reported in this paper.

References

[1] L.R. Scott, M. Vogelius, Norm estimates for a maximal right inverse of the divergence operator in spaces of piecewise polynomials, RAIRO Modél. Math. Anal. Numér. 19 (1) (1985) 111–143.

- [2] J. Qin, On the convergence of some low order mixed finite elements for incompressible fluids (Ph.D. thesis), Citeseer, 1994.
- [3] J. Qin, S. Zhang, Stability and approximability of the P1-P0 element for Stokes equations, Internat. J. Numer. Methods Fluids 54 (5) (2007) 497–515.
- [4] D.N. Arnold, J. Qin, Quadratic velocity/linear pressure Stokes elements, in: Advances in Computer Methods for Partial Differential Equations, Vol. 7, 1992, pp. 28–34.
- [5] S. Zhang, A new family of stable mixed finite elements for the 3D Stokes equations, Math. Comp. 74 (250) (2005) 543-554.
- [6] S. Zhang, On the P1 Powell-sabin divergence-free finite element for the Stokes equations, J. Comput. Math. (2008) 456-470.
- [7] S. Zhang, A family of 3D continuously differentiable finite elements on tetrahedral grids, Appl. Numer. Math. 59 (1) (2009) 219–233.
- [8] J. Guzmán, M. Neilan, Conforming and divergence-free Stokes elements in three dimensions, IMA J. Numer. Anal. 34 (4) (2014) 1489–1508.
- [9] J. Guzmán, M. Neilan, Inf-sup stable finite elements on barycentric refinements producing divergence–free approximations in arbitrary dimensions, SIAM J. Numer. Anal. 56 (5) (2018) 2826–2844.
- [10] S. Zhang, Quadratic divergence-free finite elements on Powell-sabin tetrahedral grids, Calcolo 48 (3) (2011) 211-244.
- [11] J. Guzmán, A. Lischke, M. Neilan, Exact sequences on Powell-Sabin splits, Calcolo 57 (2) (2020) 1-25.
- [12] J. Guzman, A. Lischke, M. Neilan, Exact sequences on worsey-farin splits, 2020, arXiv preprint arXiv:2008.05431.
- [13] V. Girault, P.-A. Raviart, Finite Element Methods for Navier-Stokes Equations. Theory and Algorithms, Vol. 5, Springer, 1986.
- [14] M.J.D. Powell, M.A. Sabin, Piecewise quadratic approximations on triangles, ACM Trans. Math. Software 3 (4) (1977) 316–325.
- [15] M.-J. Lai, L.L. Schumaker, Spline Functions on Triangulations, Cambridge University Press, 2007.
- [16] C. Manni, H. Speleers, Standard and non-standard CAGD tools for isogeometric analysis: a tutorial, in: Isogeometric Analysis: A New Paradigm in the Numerical Approximation of PDES, in: Lecture Notes in Math., vol. 2161, Springer, Cham, 2016, pp. 1–69.
- [17] J. Guzmán, L. Scott, The scott-vogelius finite elements revisited, Math. Comp. 88 (316) (2019) 515-529.
- [18] D. Boffi, J. Guzman, M. Neilan, Convergence of Lagrange finite elements for the maxwell eigenvalue problem in 2D, 2020, arXiv preprint arXiv:2003.08381.
- [19] L.R. Scott, S. Zhang, Finite element interpolation of nonsmooth functions satisfying boundary conditions, Math. Comp. 54 (190) (1990) 483–493
- [20] A. Worsey, G. Farin, An n-dimensional Clough-Tocher interpolant, Constr. Approx. 3 (1) (1987) 99–110.
- [21] A. Lischke, Exact smooth piecewise polynomials on Powell-Sabin and Worsey-Farin splits (Ph.D. thesis), Division of Applied Mathematics, Brown University, 2020.
- [22] P. Alfeld, A trivariate clough-tocher scheme for tetrahedral data, Comput. Aided Geom. Design 1 (2) (1984) 169-181.
- [23] D.S. Malkus, Eigenproblems associated with the discrete LBB condition for incompressible finite elements, Internat. J. Engrg. Sci. 19 (10) (1981) 1299–1310.
- [24] M. Crouzeix, P. Raviart, Conforming and non-conforming finite element methods for solving the stationary Stokes equations, RAIRO Anal. Numer. 7 (1973) 33–76.
- [25] S.C. Brenner, L. Scott, The Mathematical Theory of Finite Elements Methods, Vol. 3, Springer, 2007.
- [26] U. Trottenberg, C. Ulrich Trottenberg, C. Oosterlee, A. Schuller, A. Brandt, P. Oswald, K. Stüben, Multigrid, Elsevier Science, 2001.
- [27] D. Silvester, A. Wathen, Fast iterative solution of stabilised Stokes systems part II: Using general block preconditioners, SIAM J. Numer. Anal. 31 (5) (1994) 1352–1367.
- [28] H. Elman, V. Howle, J. Shadid, R. Shuttleworth, R. Tuminaro, A taxonomy and comparison of parallel block multi-level preconditioners for the incompressible Navier–Stokes equations, J. Comput. Phys. 227 (3) (2008) 1790–1808.
- [29] P.E. Farrell, L. Mitchell, L.R. Scott, F. Wechsung, A Reynolds-robust preconditioner for the scott-vogelius discretization of the stationary incompressible Navier-Stokes equations, The SMAI J. Comput. Math. 7 (2021) 75–96.
- [30] P.E. Farrell, M.G. Knepley, L. Mitchell, F. Wechsung, PCPATCH: software for the topological construction of multigrid relaxation methods, Trans. Math. Softw. (2021).